ELSEVIER

Coordination Chemistry Reviews
178–180 (1998) 1251–1298

COORDINATION CHEMISTRY REVIEWS

Multifunctional transition metal complexes Information transfer at the molecular level

Raymond Ziessel *, Muriel Hissler, Abdelkrim El-ghayoury, Anthony Harriman

Laboratoire de Chimie, d'Électronique et de Photonique Moléculaires,
École Européenne de Chimie, Polymères et Matériaux (ECPM), Université Louis Pasteur,
UPRES-A 7008 au CNRS, 1 rue Blaise Pascal, 67008 Strasbourg, Cedex, France

Received 30 October 1997; accepted 27 January 1998

Contents

Abstract

Recent investigations from our laboratory have described compelling experimental evidence to the effect that polyacetylenes operate as extremely effective molecular-scale wires for conducting electronic charge between redox-active terminals. The unusually low electronic resistivity of polyacetylenic bridges is derived from their relatively accessible HOMOs and LUMOs, which facilitate electron and hole tunnelling over long distances, and because of the excellent electronic coupling that occurs between adjacent carbon atoms, these being in very

---

* Corresponding author. Fax: +33 3 88 41 68 25; e-mail: ziessel@chimie.u-strasbg.fr

PII S0010-8545(98)00060-5

close proximity. In order to prevent direct participation of the acetylenic bridge in triplet energy-transfer processes or in light-induced electron-transfer reactions, it is prudent to restrict the conjugation length of the bridge to less than five ethynylene groups. We now consider various synthetic strategies for the engineering of such molecular systems that retain the favorable electronic properties of a polyacetylenic bridge but that include a relay or insulator in the bridging moiety. A convenient way to construct such systems is to use a Pt^{II} *bis*-acetylide as the spacer that separates terminal metal oligopyridine complexes. In this case, the central Pt^{II} complex becomes an insulator. By careful design of the system, this insulatory behavior can be exploited as a means by which to introduce directionality and selectivity into the system, and we demonstrate such effects by using polycyclic hydrocarbons and metalloporphyrins as the photoactive terminals. Similar effects can be obtained with polycyclic hydrocarbons built into the acetylenic wire and, in such cases, the energetics of the bridge can be tuned over an inordinately wide range by varying the extent of conjugation inherent to the aromatic nucleus. A special case is identified in which the polycycle itself possesses vacant coordination sites since the energy of the bridge can be further tuned by external complexation of adventitious cations. In order to provide for an energy gradient along the molecular axis, we have devised a versatile synthetic strategy for attaching different types of ligand to the terminals. This approach also facilitates both extension of the molecular axis and alteration of the molecular shape. The photophysical and electrochemical properties have been recorded for all the molecular systems reported herein and used as a simple experimental means by which to quantify the extent of electronic communication along the molecular axis. For mixed-metal or mixed-ligand systems, rates of intramolecular energy or electron transfer have been measured. In most cases, these rates are extremely fast and testify to the remarkable electronic coupling properties of this family of compounds. Finally, some consideration is given to the preparation of third-generation systems.

Keywords: Electron-transfer; Energy-transfer; Metal–oligopyridine complexes; Photochemistry; Polyacetylides; Molecular-scale electronics; Platinum complexes; Porphyrins

1. Introduction

For many years now we have been concerned with the design and synthesis of multicomponent molecular systems comprising discrete redox and/or photoactive subunits separated by well-defined spacer groups [1–4]. The active molecular units are selected from transition metal oligopyridine complexes, polycyclic hydrocarbons and metalloporphyrins while, in most cases, the spacer groups are short carbon chains. Of the possible types of spacer function, we have concentrated on alkynylene systems since these fulfil many of the important requisites; namely, chemical inertness, rigidity, linearity, and synthetic versatility. When compared to ethanylene and ethenylene bridges, the ethynylene units appear to be excellent electronic conductors at the molecular level [5]. Furthermore, we have shown that joining ethynylene groups into a short polyacetylene wire causes only a small attenuation in the electronic conductivity with incremental numbers of acetylenic functions [6]. This is in marked contrast to the case of polyphenyls [7–11] where electronic coupling between adjacent aromatic units is inhibited by symmetry considerations (Fig. 1).

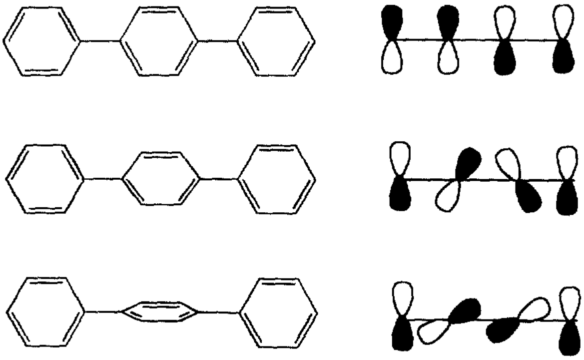

Fig. 1. Pictorial representation of orbital overlap between adjacent phenyl rings with the interaction between rings being set by their mutual orientation. The optimum angle will depend on the nature of the orbitals involved and might differ for π and π^* orbitals. Note, for metal oligopyridine complexes there might be a slight tendency for the rings to adopt a coplanar orientation upon reduction to the π-radical anion.

We conclude, therefore, that elemental carbon bridges [12–17] offer the best possibility for connecting photoactive subunits in a predetermined arrangement that provides for [modest-to-strong] electronic coupling along the molecular axis. In the current article, we restrict our attention to the design of photoactive molecular arrays. Such systems are considered to be essential components for future molecular-scale photoelectronic devices [1].

We have investigated many bi- and tripartite systems in an effort to optimize the performance of the spacer group, to identify the most useful terminal groups, and to further our understanding of how best to connect together the various units. While the carbon bridge provides structural rigidity and is an excellent conductor of both electrons and holes, we have been unable, as yet, to construct molecules longer than ca. 40 Å. One major factor that restricts extension of the molecular axis is the realization that both triplet energy and redox potential of the bridge decrease steeply with increasing chain length [18,19]. This means that no more than four acetylene groups can be oligomerized to form a bridge. Longer chain lengths introduce severe complications arising from direct participation of the bridge in subsequent photochemical or redox processes involving the active terminals (Fig. 2). To avoid such difficulties we have considered the introduction of small insulators into the carbon bridge whose function is to impose a modest barrier to electronic coupling along the molecular axis [20]. In this way, formation of polyacetylenes is avoided since the conjugated pathway can be restricted to less than four carbon atoms. This simple strategy ensures that the energies of bridge-localized HOMOs and LUMOs remain outside the range at which the bridge will interfere with electron propagation between the active subunits. This seems to us to be a better approach than simply lowering the energy of the photoactive subunits.

In searching for appropriate insulator groups we have identified, among other structural units, that Pt^{II} *bis*-σ-acetylide complexes display interesting and useful

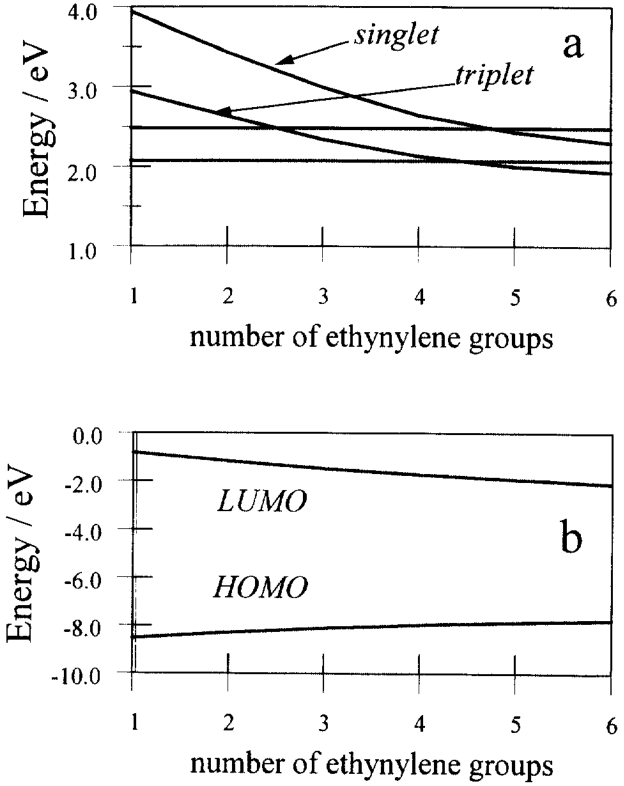

Fig. 2. Effect of chain length on the energetics of a diphenyl capped polyacetylene wire. Panel (a) shows the variation of excited singlet and triplet energies with increasing chain length compared to the approximate singlet and triplet MLCT energies of ruthenium(II) *tris*(2,2′-bipyridine). It can be seen that the energies of the LUMO and HOMO localized on the wire become lower than those of the chromophore when the chain exceeds four ethynylene groups. (b) Decrease in energy gap between LUMO and HOMO levels with increasing chain length. All calculations were made at the restricted Hartree–Foch ab initio level after energy minimization of the optimum conformation with the Gaussian-94 set of programs.

properties when used as connectors for metal oligopyridine complexes [21,22]. Such organometallic fragments, being square planar [23], usually form both *cis* and *trans* geometries that do not interconvert at reasonable temperatures nor under prolonged exposure to visible light. The auxiliary ligands coordinated to the Pt^{II} center can be selected from an inordinately wide range of readily accessible functional groups, including triarylphosphines. The latter ligands, in particular, permit facile modulation of the electronic properties of the Pt^{II} *bis*-σ-acetylide simply by perturbing the electron density at the bound phosphorus atom. These ligands increase the solubility of the final multicomponent array while maintaining the energy of the Pt^{II} *bis*-σ-acetylide at an acceptably high level.

Other ways to introduce insulatory properties into the bridge are also under active consideration and are reviewed here. In particular, we have explored the effects of incorporating a polycyclic hydrocarbon in the center of the wire [1,24] in such a way that mutual coupling between aryl rings is avoided. This type of insulator is attractive because of the simplicity with which its local energetics can be tuned. A special case arises when a chelating heterocycle is used in place of the interspersed polycycle since the local energetics can be modulated by selective complexation of added cations to the vacant ligand. This allows both extension of the molecular axis and subtle variation of the molecular or electronic properties (Fig. 3).

In this review we focus attention on recent progress made in our laboratory regarding the assembly of photoactive multicomponent systems comprising a short polyacetylenic bridge containing adventitious structural units. The objective of this work is to explore the possibility of employing such structural attributes to modify the electronic conductivity inherent to polyacetylenes in a controlled fashion. Since the acetylenic bridge is a non-passive component [12–17], it is important to learn how best to incorporate these units into the emerging supermolecule so as to benefit from their unique properties. We note that, whereas there are many descriptions of purely organic bridges, the application of organometallic units to interconnect active subunits has received scant attention. Certainly, the design elements of such molecular-scale bridges remain completely unnavigated.

2. Background

The design and construction of organometallic materials based on the stepwise acretion of acetylenic modules into a well-ordered linear array [25] is an active area of research due, in the main, to their possible application to information technology, especially in the form of molecular-scale photoelectronic devices [1]. Indeed, the isolation of putative molecular-scale wires built from oligomeric assemblies of unsaturated sequences represents an attractive synthetic target that allows evaluation of the extent of electronic coupling between remote organometallic centers to be made

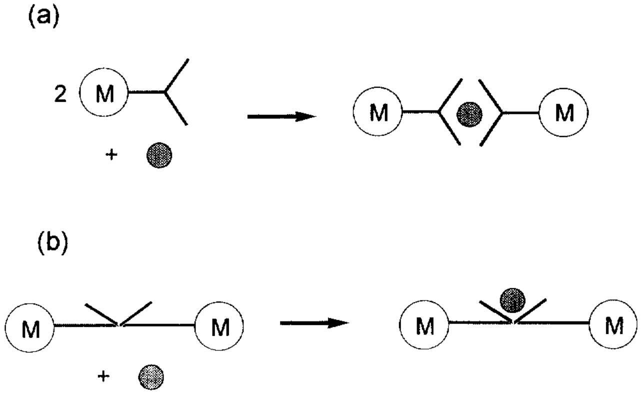

Fig. 3. Schematic representation of how complexation of a metal cation (shaded sphere) can promote (a) extension of the molecular axis and (b) perturbation of the energetics of the bridge.

at a fundamental level. Within a rough generalization, supermolecules consisting of terminal metal complexes connected by elemental carbon bridges can be divided into three main categories according to how the bridge is joined to the metal center.

(i) The acetylenic function can be attached directly to the metal center [26–28], providing access to structures in which the neutral bridge can adopt several extreme mesomeric forms; i.e. polyyne-like (I), cumulene-like (II), polycarbyne-like (III), and hybrid systems (IV, V, etc).

$\mathrm{M{-}(C{\equiv}C)_n{-}M}$

I

$\mathrm{M(=C=)_nM}$

II

$\mathrm{M{\equiv}C(C{\equiv}C)_nC{\equiv}M}$

III

$\mathrm{M{=}C(C{\equiv}C)_nM}$

IV

$\mathrm{M{=}C(C{\equiv}C)_nC{=}M}$

V

(ii) The acetylene group can be covalently linked to chelating fragments that are coordinated to the metal center [29,30]. In such structures it is normal to distinguish between coordinating ligand and alkynylene bridge but these entities may be sufficiently coupled to render such distinction a somewhat hazardous process.

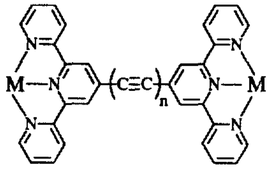

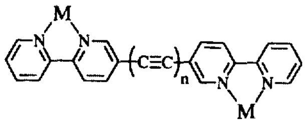

(iii) The acetylene function can be attached to a coordinating ligand at one end and directly to a metal center at the opposite end, giving rise to hybrid systems [21]. A key function of such molecular modules concerns the formation of a stable metal-to-σ alkynyl bond.

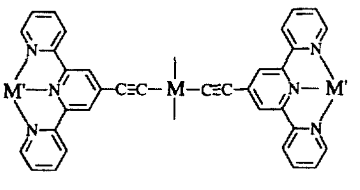

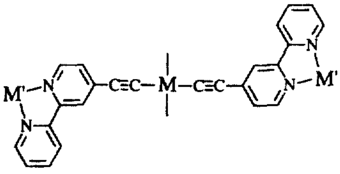

The first class of compounds has evolved rapidly over the last few years or so due to the efforts of several research groups [31–36]. Extended molecular systems are now available that contain up to 20 carbon atoms in the alkynylene bridge and for which the redox-active organometallic terminal groups are activated at relatively low potential. Significant interaction between the termini has been reported for mixed-valence complexes [37,38] even with bridges containing as many as 11 carbon atoms. Charge transfer along such capped chains has been probed by cyclic voltammetry but, on extending the carbon chain, the magnitude of interaction between the organometallic terminals decreases quite rapidly. More recently, molecules of this type have been used for the preparation of soluble polymers and as models of conductive networks [39]. Attempts have also been made to introduce a metallo-fragment as chromophore [40].

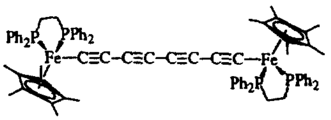

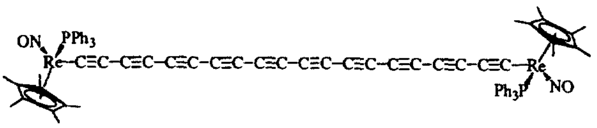

The second class of molecules has been reviewed recently [1–4]. It appears that alkynylene bridges actively promote long-range electronic coupling between remote redox- and photoactive units [5,6,41], especially when triggered by external visible-light stimulation. Intramolecular triplet energy transfer, photon migration, and light-induced electron transfer occur by way of rapid through-bond electronic processes for which the rate decreases only slightly with increasing length of the connecting carbon bridge. In the special case where the terminal groups are ruthenium(II) or osmium(II) oligopyridine complexes, it has been shown that facile electron delocalization over an extended π^* orbital takes place within the triplet manifold [42–46]. This process extends the triplet lifetime, in certain cases by a factor of ca. 3000-fold, thereby increasing the probability that the excited state can participate in chemical reactions [43].

We have recently developed the third class of compound in which a luminophore is used as the capping group for a Pt^{II} *bis*-σ-acetylide complex [47]. Two complementary synthetic methodologies have been introduced: the first procedure involves exposure of σ-alkynyl-bipyridine or terpyridine metallo-ligands of platinum(II) to a preformed metal precursor containing adequate molecular fragments to complete the coordination sphere around the metal (Fig. 4); the second procedure involves the use of functionalized metallo-synthons bearing an ethynyl or pseudo-halide group with the $[Pt(^nPBu_3)_2Cl_2]$ precursor in cross-coupling reactions. This novel strategy provides access to heterodinuclear complexes in a highly controlled manner (Fig. 5).

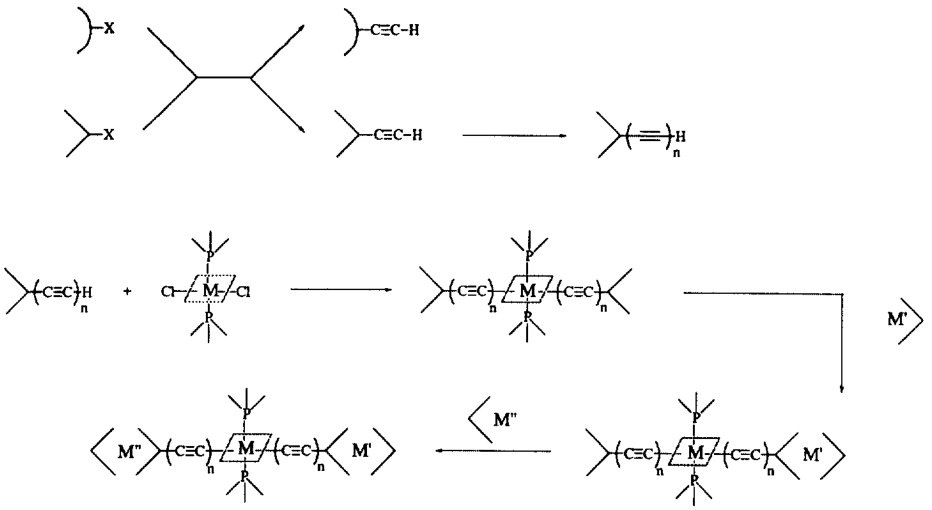

Fig. 4. General synthetic scheme used to prepare Pt^{II} *bis*-acetylide bridged metallo-ditopic ligands and their M′, M″ transition metal complexes.

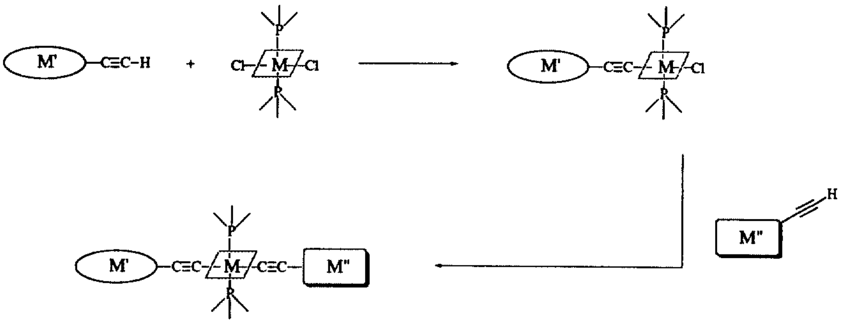

Fig. 5. General synthetic scheme used to prepare Pt^{II} *bis*-acetylide bridged, mono- and binuclear metallo-complexes starting from a functionalized metal complex.

3. σ-Alkynyl metallo-ligands

A major problem associated with the future development of photoactive molecular-scale wires concerns the question of how to modulate the energetics of the carbon bridge versus that of the terminal units. Varying the energy of these terminal units is easy but it is far from obvious how to tune the electronic properties of the connecting spacer moiety. At an early stage of this project, however, we noted an important effect that suggested it will become possible to control the degree of electronic coupling along the bridge by simple synthetic means [42]. Thus, the strong electronic coupling that persists between the terminal units of polyacetylene-bridged binuclear metal oligopyridine complexes is essentially lost upon insertion of a phenyl ring between pyridine and acetylene functions. This curtailment of electron flow is due to poor alignment of orbitals on adjacent pyridine and phenyl functions due to unfavorable orientation of the rings [7–11]. This has the effect of decreasing orbital overlap at the connecting point and we sought to exploit the effect by introducing different aromatic residues into the polyacetylene bridge. However, the barrier arises only when two or more aryl rings are coupled together and we found no undue barrier for connecting a single aryl ring to an acetylene.

A slightly different variation on this theme, that does provide the required effect, is to incorporate a "Pt(^{n}Bu$_3$P)$_2$" core between the bpy–C≡C–C≡C–bpy pontoon [21,22]. Subsequent complexation of the diimine system by suitable luminophoric d^6-metal centers provides access to an unusually wide range of photoactive molecular dyads whose properties differ markedly from those of the corresponding alkynylene-bridged complexes. We now concentrate on the synthesis and properties of this new class of photoactive supermolecules.

4. Synthesis of σ-alkynyl metallo-ligands

Oligopyridines functionalized with one and/or two alkyne substituents [48] have been connected to a square-planar platinum(II) complex using a CuI catalyst and diisopropylamine as base [21]. In particular, this synthetic strategy facilitates the isolation of linear bipyridine derivatives **1** or of the corresponding L-shaped compounds **2** (Fig. 6) via clean and stereospecific reactions. Of course, the site at which the alkyne is attached to the pyridine ring can be varied between the 4-, 5-, and 6-positions while several alkynes can be attached to the same bipyridine. Furthermore, the synthetic approach is readily modified so as to produce the ana-

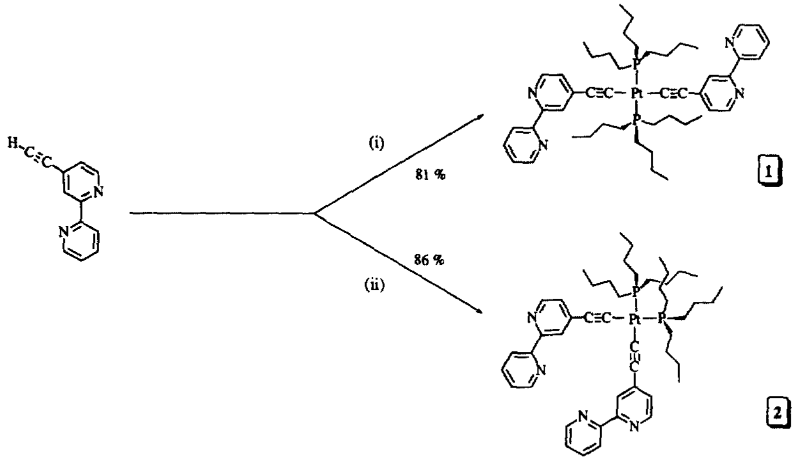

Fig. 6. Synthesis of "linear" (**1**) and "bent" (**2**) Pt^{II} *bis*-σ-acetylides bearing vacant 2,2′-bipyridyl ligands suitable for subsequent complexation of incoming metallo-fragments: (i) *trans*-[Pt^{II}(^{n}Bu$_3$P)$_2$Cl$_2$], CuI (ca. 1 mol%), (^{i}Pr)$_2$NH, THF, 25 °C, 5 days; (ii) *cis*-[Pt^{II}(^{n}Bu$_3$P)$_2$Cl$_2$], CuI (ca. 1 mol%), (^{i}Pr)$_2$NH, THF, 25 °C, 5 days.

logous terpyridine compounds **3**–**5** (Fig. 7). These latter compounds are attractive because the alkyne is attached to the central pyridine ring of the coordinating ligand in such a way as to favor generation of rigid and linear molecular arrays.

Exposure of these metallo-ligands to a preformed metallo-precursor that possesses the molecular fragments necessary to complete the coordination shell of the metal [e.g. $M(bpy)_2Cl_2$, M = Ru or Os] provides a direct route by which to access multicomponent heteropolynuclear complexes (Fig. 8). An interesting, if not [in the context of molecular model building] essential, feature of this synthetic modality concerns the ability to prepare both symmetrical binuclear complexes, such as *trans*-RuPtRu, and the corresponding mononuclear complex **7**. The latter can be functionalized so as to produce asymmetrical binuclear complexes, such as *trans*-RuPtOs, suitable for studying intramolecular triplet energy transfer across the central Pt^{II} *bis*-σ-acetylide spacer. This *trans*-RuPtOs complex could indeed be prepared in improved yield starting from the corresponding *trans*-OsPt complex. The mononuclear Ru complex can also be assembled around a reactive metal center so as to form heptanuclear complexes, such as Ru_3Pt_3Fe **9**, that facilitate the study of energy transfer from the peripheral chromophores to the central unit [21]. By analogy, the *cis*-RuPtOs complex can be prepared [22] as illustrated in Fig. 9. It is noteworthy that the resultant complexes are kinetically stable in solution, resistant to thermal and photochemical isomerization as evidenced by NMR and IR spectroscopy, and facilitate exact positioning of prefabricated modules into ordered arrays.

An original synthetic protocol has been used for preparation of the *cis*-RuPtRu complex **12** (Fig. 10). In parallel with the previous procedure (Figs. 6–9), we found that grafting of two [ruthenium *bis*-bpy, bpy-ethynyl] units to a platinum core via σ-ethynyl bonds is also effective in the presence of catalytic amounts of CuI. The generality of this synthetic procedure is demonstrated by the monofunctionalization

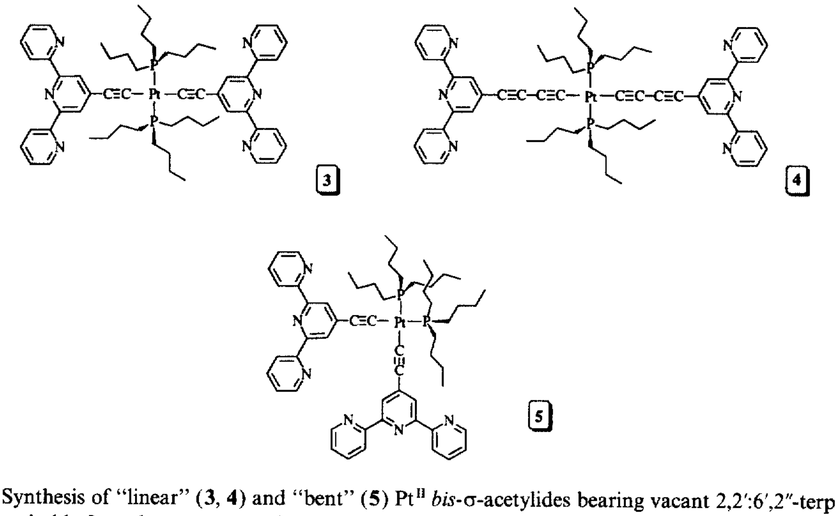

Fig. 7. Synthesis of "linear" (**3**, **4**) and "bent" (**5**) Pt^{II} *bis*-σ-acetylides bearing vacant 2,2′:6′,2″-terpyridyl ligands suitable for subsequent complexation of incoming metallo-fragments.

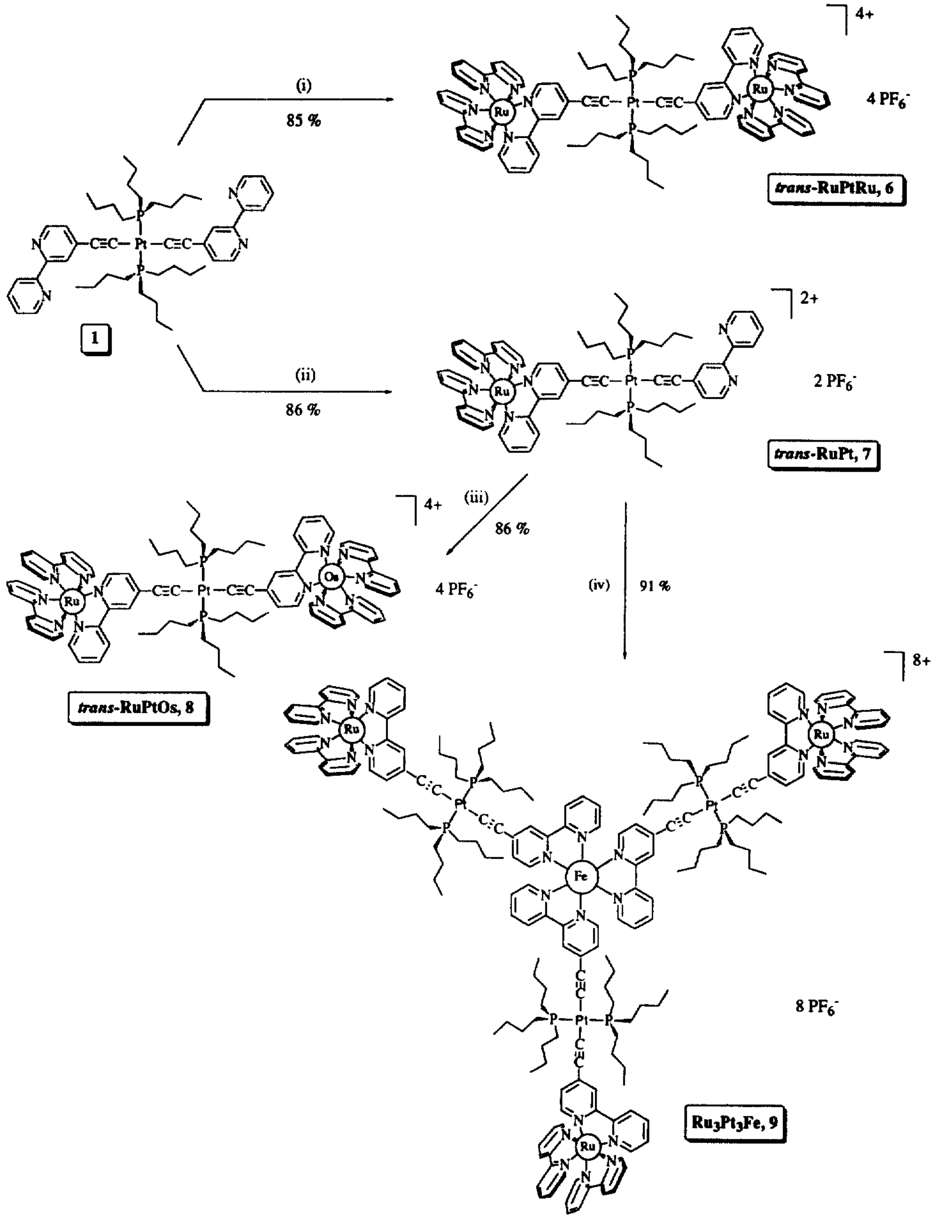

Fig. 8. Synthetic route used to prepare heteropolynuclear complexes using Pt^{II} σ-acetylides as spacers: (i) 2 equiv. [Ru(bpy)$_2$Cl$_2$]·2H$_2$O, C$_2$H$_5$OH, 80 °C, 15 h; (ii) 1 equiv. [Ru(bpy)$_2$Cl$_2$]·2H$_2$O, C$_2$H$_5$OH, 80 °C, 15 h; (iii) 1 equiv. [Os(bpy)$_2$Cl$_2$], C$_2$H$_5$OH, 90 °C, 3 days; (iv) ca. 0.4 equiv. FeSO$_4$·7H$_2$O, C$_2$H$_5$OH/H$_2$O, 25 °C, 10 min exposure to ultrasonic irradiation.

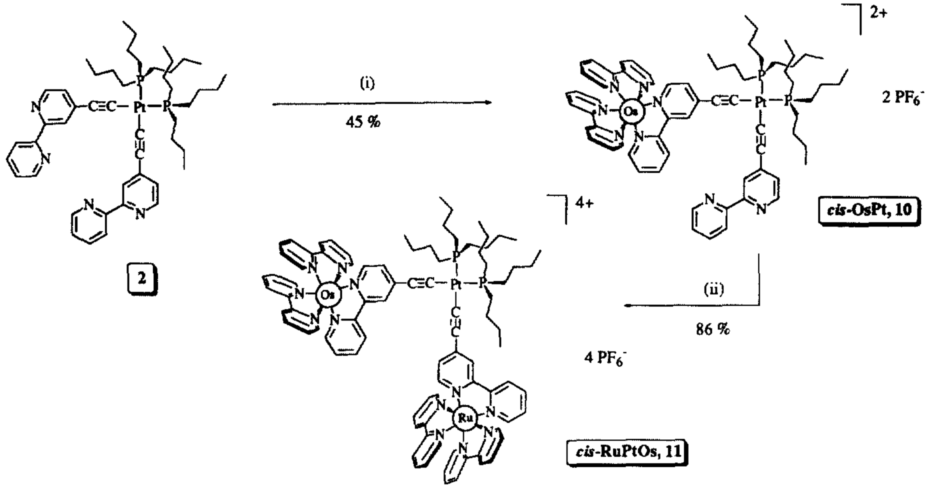

Fig. 9. Synthetic route used to prepare *cis*-RuPtOs (**11**): (i) 1 equiv. [Os(bpy)$_2$Cl$_2$], C_2H_5OH, 80 °C, 3 days; (ii) 1 equiv. [Ru(bpy)$_2$Cl$_2$]·2H$_2$O, C_2H_5OH, 80 °C, 2 days.

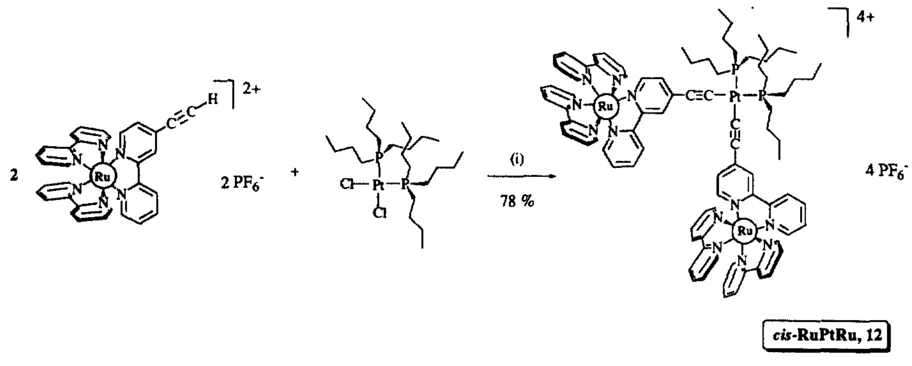

Fig. 10. Synthetic procedure followed for the preparation of *cis*-RuPtRu (**12**): (i) CuI (ca. 2 mol%), $(^i\mathrm{Pr})_2$NH, CH_3CN/THF, 25 °C, 5 days.

of the "Re(bpy)(CO)$_3$" fragment and by the difunctionalization of the "Ru(bpy)$_2$" systems. It is noteworthy that the [HC≡C–Re(bpy^{t}Bu$_2$)(CO)$_3$] complex could be dimerized by an oxidative coupling reaction (Fig. 11) [40].

5. Properties of metal complexes formed around σ-alkynyl metallo-ligands

As a direct result of the above-described research effort, a synthetic strategy is now in place that permits the construction of rigid multinuclear complexes around a Pt^{II} *bis*-σ-acetylide center. The next issue, with regard to the design of effective molecular-scale electronic devices, is to ensure that the central Pt^{II} *bis*-σ-acetylide

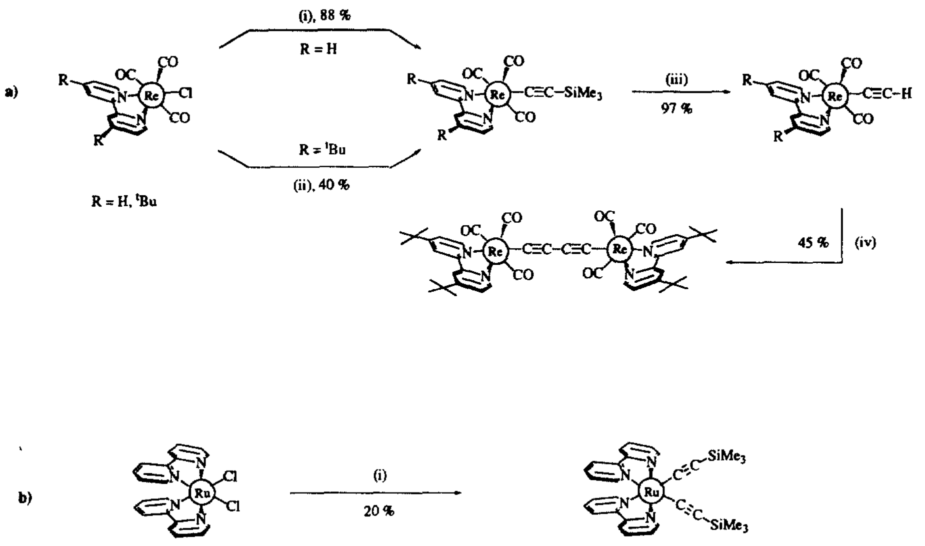

Fig. 11. Monofunctionalization of (a) Re(I) and (b) Ru(II) metallo-fragments so as to introduce a reactive ethynylene function. Subsequent coupling reactions give rise to binuclear metallo-complexes: (i) TMS–C≡C–H, CuI, CH_3CN/THF, 90 °C, 15 days; (ii) n-BuLi, TMS–C≡C–H, THF, 1 day; (iii) KOH, CH_3OH, 25 °C, 2 days; (iv) $Cu(OAc)_2$, pyridine, 60 °C, 1 day.

does not quench the excited states of the terminal metal complexes. This possibility was addressed by measuring the photophysical properties of the various mono- and binuclear complexes and making a critical comparison with the properties recorded for the parent $M(bpy)_3$ complexes under identical conditions [21,22]. Results were collected in deoxygenated media at both room temperature and 77 K.

It turns out that the central Pt^{II} *bis*-σ-acetylide does not quench the excited triplet state of any of the terminal metal complexes and, instead, there is a small enhancement in luminescence quantum yield and lifetime upon incorporation of an alkyne group. The absence of intramolecular quenching can be attributed to the relatively high energy of states localized on the Pt^{II} *bis*-σ-acetylide with respect to the terminals. Moreover, the luminescence spectra recorded for the ruthenium(II) and osmium(II) complexes (Fig. 12) are closely comparable with those recorded for the relevant parent $M(bpy)_3$ complexes. This suggests that, at the triplet level, an electron is promoted from the metal center to a π* orbital localized on one of the unsubstituted 2,2′-bipyridyl ligands rather than onto the Pt^{II} *bis*-σ-acetylide-bridged ditopic ligand. In the latter case, we would expect a substantial red-shift for the emission maximum. Similarly, the triplet–triplet absorption spectra recorded for these complexes [Fig. 12(b)] remain similar to those found for the parent complexes and lack the near-infrared absorption transition characteristic of charge injection into a highly-conjugated ditopic ligand [42,46].

Electrochemical studies [21,22] were also consistent with the notion of the unsubstituted 2,2′-bipyridyl ligand being more easily reduced than the Pt^{II} *bis*-σ-acetylide

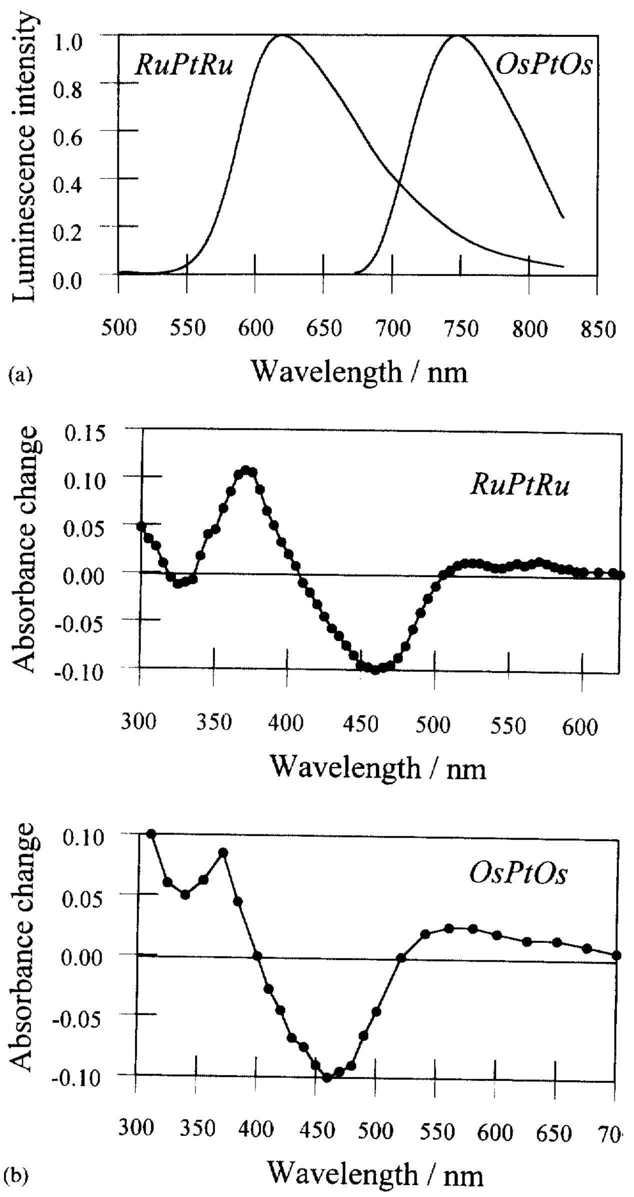

Fig. 12. (a) Luminescence and (b) differential absorption spectra recorded for the triplet excited states of *trans*-RuPtRu (**6**) and the corresponding *trans*-OsPtOs complex in deoxygenated acetonitrile. In each case, the spectrum closely resembles that recorded for the parent complex.

bridged ditopic ligand. Thus, addition of one electron to the various mono- and binuclear complexes occurs with a reduction potential very similar to that found for the parent complex. The corresponding oxidation processes are also relatively unaffected by the presence of the Pt^{II} *bis*-σ-acetylide. These cyclic voltammograms show no evidence for oxidation or reduction of the Pt^{II} *bis*-σ-acetylide. In fact, the reduction potential measured for the Pt^{II} *bis*-σ-acetylide-bridged ditopic ligand ($E_{red} = -2.02$ V vs. Ag°) is only slightly less negative than that recorded for 2,2′-bipyridine ($E_{red} = -2.06$ V vs. Ag°). In marked contrast, the ethynylene-bridged ditopic ligand is reduced much more easily ($E_{red} = -1.52$ V vs. Ag°). These findings suggest that the Pt^{II} center donates charge to the appended 2,2′-bipyridyl ligand [23], thereby lowering its reduction potential and favoring charge injection from metal center to an unsubstituted ligand in the triplet state.

The picture that emerges from these investigations is that the Pt^{II} center is more than a mere insulator since, in addition to imposing a high energy barrier to electron flow, it induces the photoactive terminal to inject charge into one of the auxiliary ligands upon illumination. This is not conducive to the development of an effective molecular wire. Confirmation of this dual-action inhibitory effect of the Pt^{II} center was sought by comparing the rates of intramolecular triplet energy transfer in asymmetrical Ru^{II}–Os^{II} complexes having a butadiynylene bridge (RuOs) and a Pt^{II} *bis*-acetylenic bridge (*trans*- or *cis*-RuPtOs) (Fig. 13). Such studies are assisted by the realization that the absorption bands due to individual chromophores are reasonably accessible in this complex.

It was found [6] that RuOs undergoes extremely fast intramolecular energy transfer from the terminal Ru^{II} fragment to its counterpart Os^{II} fragment upon excitation with visible light (Fig. 13). The rate constant for this event, being among the fastest ever measured for a triplet–triplet energy transfer process, is $3.7 \times 10^{10}\ s^{-1}$ at room temperature. Förster-type energy transfer [49], although relatively favorable for this complex, cannot account for such a high rate of energy transfer so that the mechanism most likely corresponds to Dexter electron-exchange [50]. This mechanism involves simultaneous electron (through LUMOs) and hole (through HOMOs) transfer involving orbitals resident on the acetylenic bridge [51]. In terms of Marcus theory [52,53], the electronic coupling matrix element describing triplet energy transfer is estimated to be ca. $12\ cm^{-1}$ for a metal-to-metal separation of ca. 16.2 Å. Triplet energy transfer in this system, for which the energy gap is 0.11 eV, is promoted by several important factors. These may be summarized as follows.

(i) Selective charge injection into the ditopic ligand upon illumination into the Ru^{II} polypyridine complex.

(ii) Extensive electron delocalization over a π* orbital encompassing much of the ditopic ligand.

(iii) A high conductivity of the ditopic ligand for both electron and hole transfer [2,3].

Intramolecular triplet energy transfer in *trans*-RuPtOs [22] occurs much more slowly (Fig. 13). The rate constant measured for this process, $k_{TT} = 1.3 \times 10^7\ s^{-1}$, is not much higher than the calculated rate constant for Förster-type energy transfer, $k_F = 1.8 \times 10^6\ s^{-1}$. This suggests that both dipole–dipole (i.e. through-space) and electron-exchange (i.e. through-bond) mechanisms are operating in this system. Relative to RuOs, the energy gap ($\Delta E = 0.35$ eV) is more substantial while the metal-

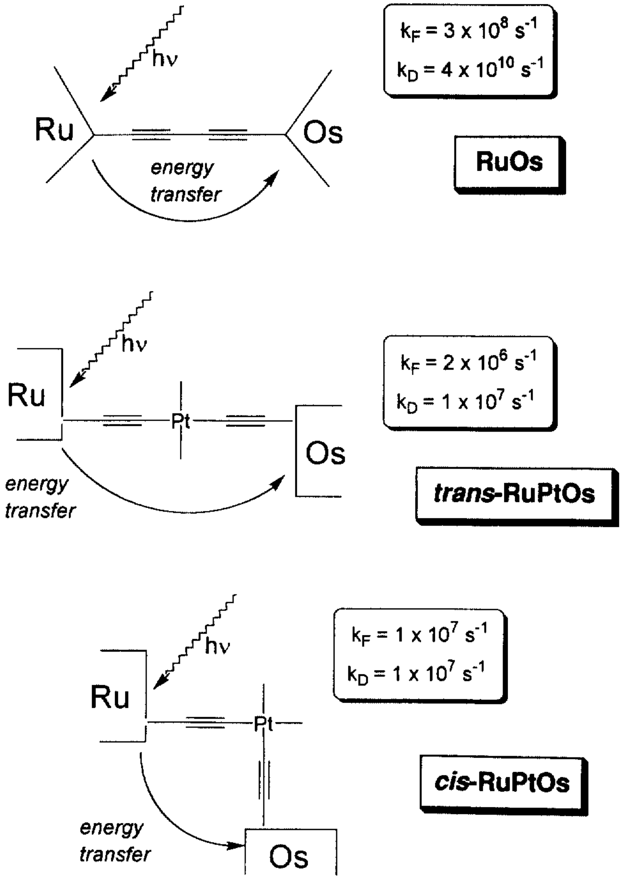

Fig. 13. Pictorial comparison of the triplet energy transfer processes that occur in the various RuOs mixed-metal complexes. Shown are the calculated rate constants (k_F) for Förster-type dipole–dipole energy transfer and corresponding rate constants (k_D) for Dexter-type electron exchange. The systems compared are the butadiynylene-bridged terpyridyl complex and the Pt^{II} *bis*-σ-acetylide bridged species **8** and **11**.

to-metal separation ($d = 19.2$ Å) is only a little larger. Taking the calculated Förster rate as being accurate, the rate constant for electron exchange ($k_D = 1.1 \times 10^7\ s^{-1}$) is some 3000-fold smaller than that measured for RuOs while the electronic coupling matrix element for through-bond electron exchange is estimated to be $< 0.2\ cm^{-1}$.

The rate of triplet energy transfer is even slower in the corresponding *cis*-RuPtOs complex [22], where $k_{TT} = 1.0 \times 10^7\ s^{-1}$ (Fig. 13). In this case, triplet energy transfer could be explained entirely in terms of the Förster mechanism ($k_F = 1.2 \times 10^7\ s^{-1}$) because of the shorter metal-to-metal separation ($d = 13.7$ Å). For the *cis* geometry, through-bond electron exchange is further restricted by poor orbital overlap around the Pt^{II} *bis*-σ-acetylide.

These experiments serve to indicate the dramatic curtailment in through-bond electronic coupling that occurs when a Pt^{II} *bis*-σ-acetylide complex is built into the bridge. The highly effective electronic coupling that is inherent to polyacetylenes [6,41] is lost while the ability of an alkyne substituent to direct charge injection selectively into the substituted ligand is overcome. The net result is that the Pt^{II} *bis*-σ-acetylide bridge does not operate as a molecular-scale wire, at least in these systems. Because this molecular module offers many significant synthetic attributes [54–57], such as the ability to form linear and bent geometries at will, we decided to further explore its electronic conductivity in the hope of avoiding the above-mentioned difficulties. This formidable challenge required replacing one or more of the terminal metal complexes with a different photoactive unit.

6. Changing the terminal subunits

As described above, incorporation of a Pt^{II} *bis*-σ-acetylide complex into a polyacetylenic bridge slows the rate of intramolecular electron exchange to an unacceptable extent. From the studies made to date it is not possible to resolve the exact cause of this inhibition of electron flow because of competing effects induced by the presence of the Pt^{II} *bis*-σ-acetylide. Thus, the central Pt^{II} *bis*-σ-acetylide increases the distance over which electrons must tunnel, because of the propensity to direct charge injection into the auxiliary ligands, and imposes an additional barrier by way of its high HOMO and LUMO. In an effort to better understand which of these two effects is responsible for the slow rate of electron exchange across the Pt^{II} *bis*-σ-acetylide bridge, we have studied compounds having quite different terminal groups.

The modular engineering of such novel systems demands the precise positioning of prefabricated units of quite disparate nature around a central metallic core [58]. One approach to this problem, developed recently in our laboratory, is based on the monofunctionalization of $[Pt(^{n}Bu_3P)_2Cl_2]$ by attachment of the first building block via a σ-alkynyl bond (Fig. 14). Subsequent attachment of a different group in place of the remaining chloride ligand allows stepwise construction of multicomponent molecular systems. The first selected example is shown in Fig. 14, where a zinc porphyrin and a "Ru(bpy)$_3$" unit are covalently linked to the central platinum core via acetylenic bonds. In this case, the Pt^{II} *bis*-σ-acetylide bridge remains in the *trans* configuration. Note the presence of a phenyl ring between porphyrin nucleus and the Pt^{II} *bis*-σ-acetylide. This ring is intended to minimize charge transfer from the Pt^{II} center to the porphyrin [23]. Again, the phosphine groups assist solubility of the assembled compound.

This synthetic methodology permits the facile connection of a metalloporphyrin to a metal *tris*(2,2′-bipyridyl) complex at a center-to-center separation of ca. 23 Å. The two terminal cations can be easily exchanged so that a wide range of mixed-metal systems can be generated having different energetics. Again, the site at which the alkyne is attached to the terminal units can be varied while the geometry and ligand field around the central Pt^{II} *bis*-σ-acetylide can be modified. The resultant complexes are rigid, structurally well-defined, and highly stable. There are, in fact,

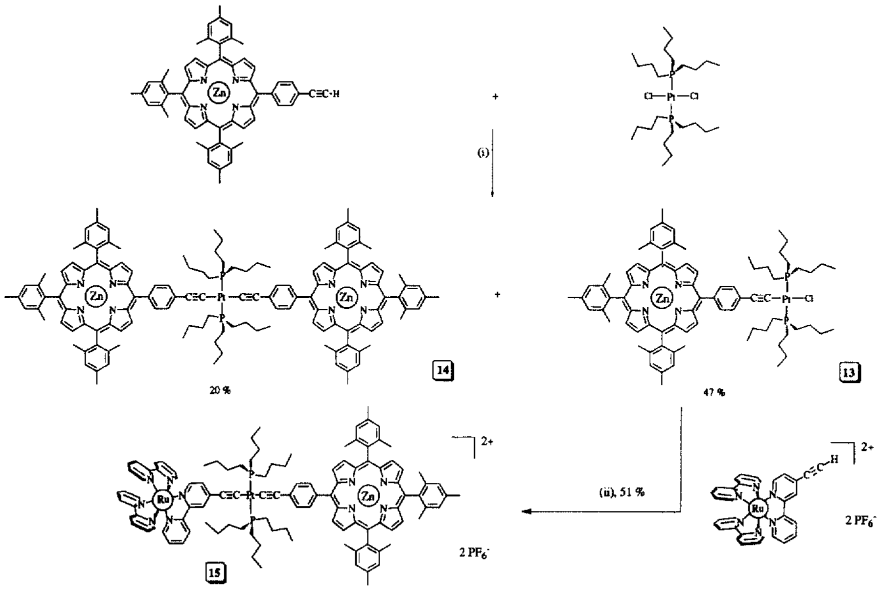

Fig. 14. Synthetic route used to prepare the mono- (**13**) and binuclear (**14**) ZnP derivatives containing a Pt^{II} σ-acetylide function as substituent or bridge. The mononuclear complex **13** is used in subsequent reactions to prepare the ZnP–Pt^{II}–Ru^{II} tripartite complex **15**: (i) CuI (1 mol%), $(^iPr)_2NH$, THF, 25 °C, 7 days; (ii) CuI (1 mol%), $(^iPr)_2NH$, CH_3CN/THF, 25 °C, 3 days.

very few systems that combine photoactive porphyrins and transition metal chelates into a single molecular entity [59–63]. This is an appealing system because of the complementary chromophoric properties of porphyrin and metal complex (Fig. 15). In such systems, according to the exact nature of the selected cations, a variety of intramolecular energy and electron transfer steps can be expected to take place under selective illumination into one of the chromophores. It becomes interesting, therefore, to explore the effects of the Pt^{II} *bis*-acetylide bridge on these various processes.

In the second example, the terminal metalloporphyrin is replaced with a polycyclic hydrocarbon, with preparation of a mixed *trans*-pyrene–Pt–Ru$(bpy)_3$ complex being illustrated in Fig. 16. By making use of tin chemistry it becomes possible to avoid basic conditions, which otherwise present problems in this synthetic procedure. Reaction results in exclusive isolation of those compounds having a *trans*-Pt^{II} *bis*-σ-acetylide bridge, such as the *trans*-*bis*-pyrene derivative **18**, even if the precursor was the *cis*-Pt^{II} *bis*-σ-acetylide complex.

In fact, the analogous *cis*-pyrene compounds could not be prepared in this way, probably because of the strong *trans*-effect induced by the pyrene fragment versus the π-acceptor character of an oligopyridine. Interestingly, the mono-terpy *cis*-complex could be synthesized in the presence of CuCl, but attachment of the ethynyl–pyrene subunit caused isomerization to the *trans*-terpy–Pt–pyrene species as deduced by ^{31}P NMR [Fig. 17(a)]. Confirmation that some type of *trans*-effect

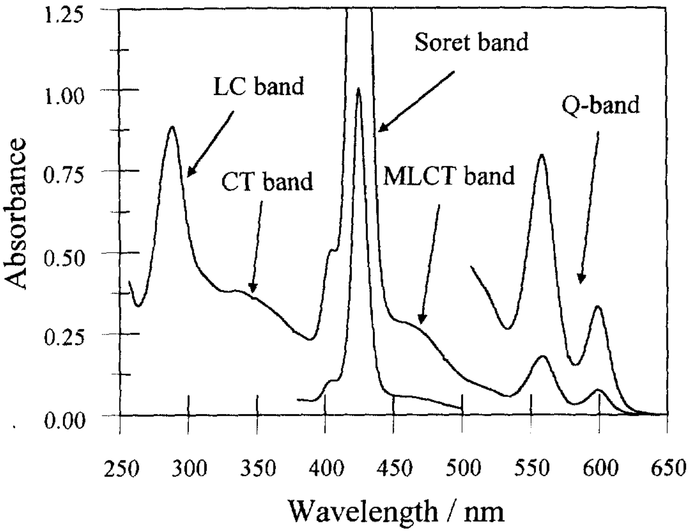

Fig. 15. Absorption spectrum recorded for the ZnP–Pt^{II}–Ru^{II} tripartite complex (**15**) in acetonitrile solution with the important transitions being labelled. The Q- and Soret bands are associated with ZnP while the MLCT (metal-to-ligand, charge-transfer) and LC (ligand-centered) bands belong to the terminal ruthenium(II) *tris*(2,2′-bipyridyl) complex. The CT (charge-transfer) band is due to charge transfer from the central Pt^{II} *bis*-acetylide to the covalently-linked 2,2′-bipyridyl ligand.

operates in these pyrene compounds is seen by examination of Fig. 17(b), where the *trans*-mono-pyrene species is obtained from the *cis*-platinum precursor.

Our interest in using photoactive polycyclic hydrocarbons as the terminal groups [64] arises, in part, from the realization that these units provide easy access to high-energy but long-lived excited singlet states. It seems reasonable to suppose that these excited states will lie closer in energy to orbitals localized on the Pt^{II} *bis*-σ-acetylide bridge than do the triplet states of the metal complexes and, consequently, they are more able to promote electron (or hole) tunnelling through the bridge [65–67]. A second important factor is that these polycycles are likely to compete with the terminal 2,2′-bipyridyl ligand as an acceptor for charge donation from the central Pt^{II} complex. Such strong charge-transfer interactions will modulate the electronic properties of the Pt^{II} *bis*-σ-acetylide bridge, perhaps facilitating direct involvement of the Pt^{II} species in redox processes. In this way, the insulating character of the bridge might be short-circuited.

7. The porphyrin–Pt–Ru(bpy)$_3$ system

The absorption spectrum recorded for the tripartite system comprising terminal zinc porphyrin (ZnP) and ruthenium(II) *tris*(2,2′-bipyridyl) units linked via a Pt^{II} *bis*-acetylide shows that the chromophores of each component are quite well resolved (Fig. 15). The ZnP exhibits moderately strong Q-band transitions around

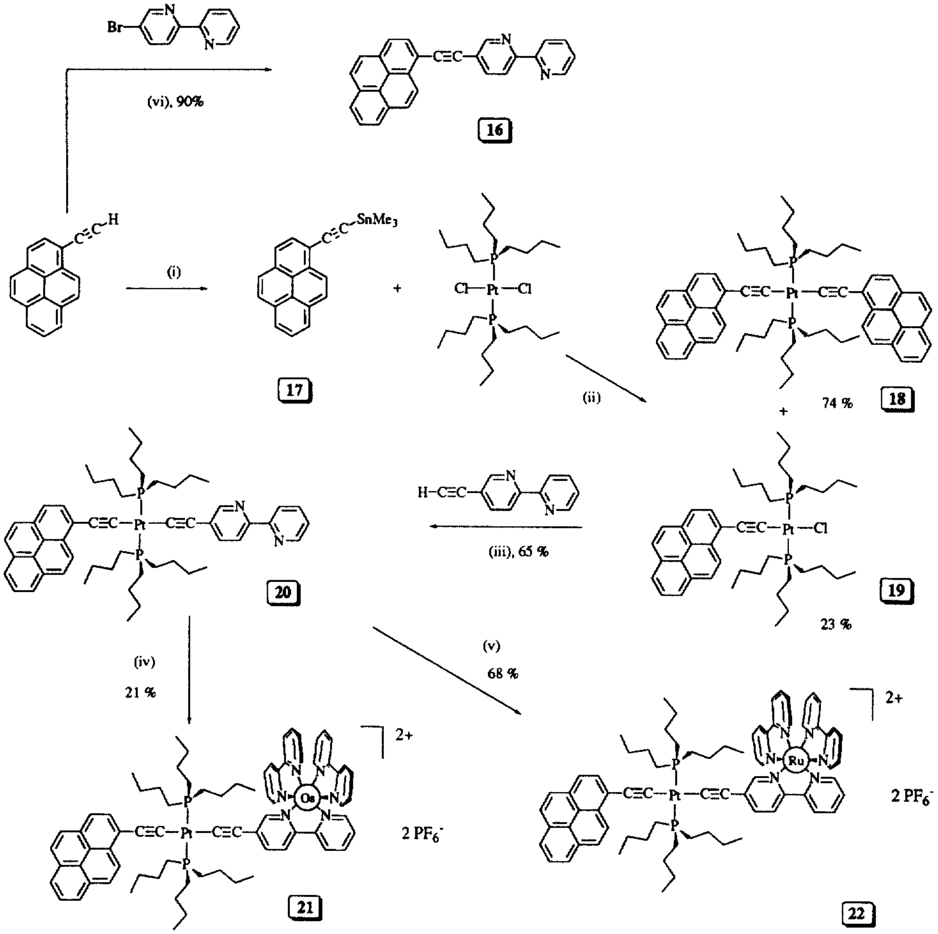

Fig. 16. Synthetic route used to attach one (**19**, **20**) or two (**18**) pyrene units to a central Pt^{II} *bis*-acetylide. The mono-derivative (**19**) is the key intermediate for further functionalization to give the Ru–Pt–pyrene (**22**) and Os–Pt–pyrene (**21**) photoactive dyads. These latter compounds require isolation of the important building block **20** that contains a vacant 2,2′-bipyridine ligand: (i) (a) n-BuLi, THF, −78 °C, 2 h, (b) $SnMe_3Cl$; (ii) CuI (1 mol%), THF, 60 °C, 2 days; (iii) CuI (1 mol%), $(^iPr)_2NH$, THF, 25 °C, 5 days; (iv) 1 equiv. $[Os(bpy)_2Cl_2]$, C_2H_5OH, 80 °C, 1 day; (v) 1 equiv. $[Ru(bpy)_2Cl_2]\cdot 2H_2O$, C_2H_5OH, 80 °C, 1 day; (vi) $[Pd^0(PPh_3)_4]$ 6 mol%, C_6H_6, $(^iPr_2)NH$, 80 °C, 15 h.

550–600 nm and a very intense Soret band at 422 nm, whereas the metal-to-ligand charge-transfer (MLCT) absorption transition centered on the ruthenium(II) *tris*(2,2′-bipyridyl) fragment is clearly visible in the range 440–500 nm. Furthermore, the Pt^{II} *bis*-σ-acetylide shows a charge-transfer transition in the near UV region [21,23] that appears as a shoulder on the more intense π, π* transitions associated with the 2,2′-bipyridyl ligands. This level of resolution is sufficient to study the various processes that take place under selective illumination in deoxygenated acetonitrile at 20 °C.

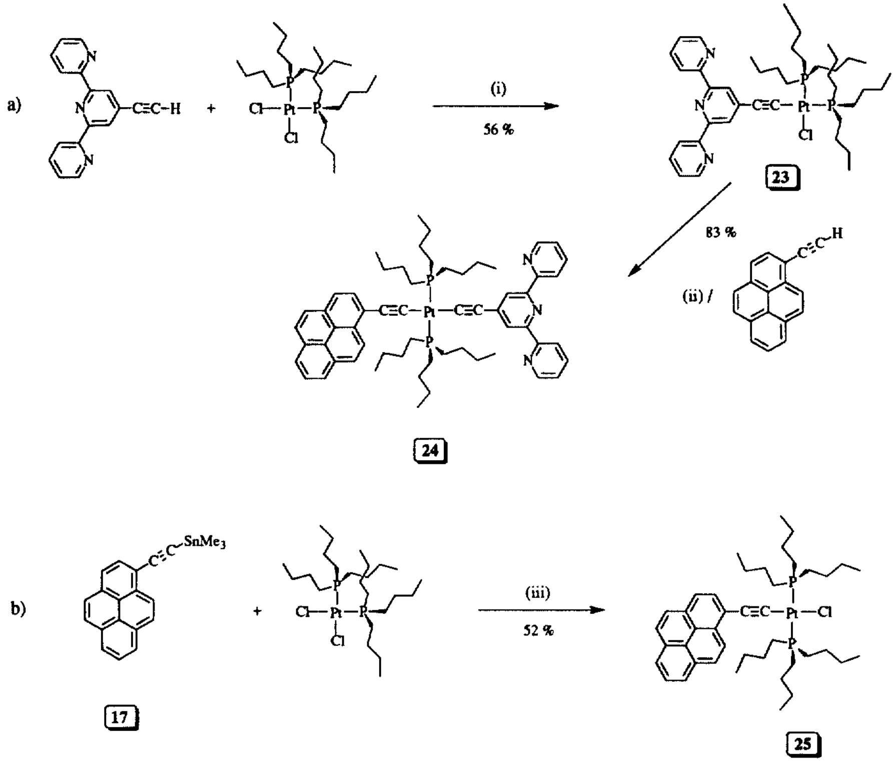

Fig. 17. Illustration of the isomerization that occurs around the Pt^{II} center upon attachment of a pyrene derivative. Such reactions, using classical conditions, always give rise to the *trans* geometry: (i) CuCl (1 mol%), THF, 25 °C, 2 h; (ii) CuI (1 mol%), THF, 60 °C, 5 days; (iii) CuI (1 mol%), THF, 60 °C, 8 days.

For the symmetrically substituted reference compound (**14** in Fig. 14) it was shown [22] that direct illumination into the charge-transfer absorption bands associated with the central Pt^{II} *bis*-σ-acetylide results in rapid and quantitative energy transfer to the terminal units. Thus, the central organometallic fragment operates as a light-harvesting unit for UV photons.

Illumination into the MLCT transition localized on the terminal ruthenium(II) *tris*(2,2′-bipyridyl) fragment gives rise to extremely weak luminescence characteristic of the triplet excited state of this unit [68]. In fact, the measured triplet lifetime is only ca. 17 ns, compared to a value of ca. 1 μs recorded for the appropriate reference compounds. This finding indicates that the excited triplet state of the terminal ruthenium(II) *tris*(2,2′-bipyridyl) fragment is extensively (i.e. >95%) quenched in the tripartite system. Detailed examination of the photophysical properties of this system has allowed evaluation of the overall photon balance such that rate constants can be derived for the various quenching steps (Fig. 18). It appears that triplet-to-singlet energy transfer to the appended ZnP, this being a spin-forbidden process [69], occurs by way of the Förster-type dipole–dipole mechanism, with a rate

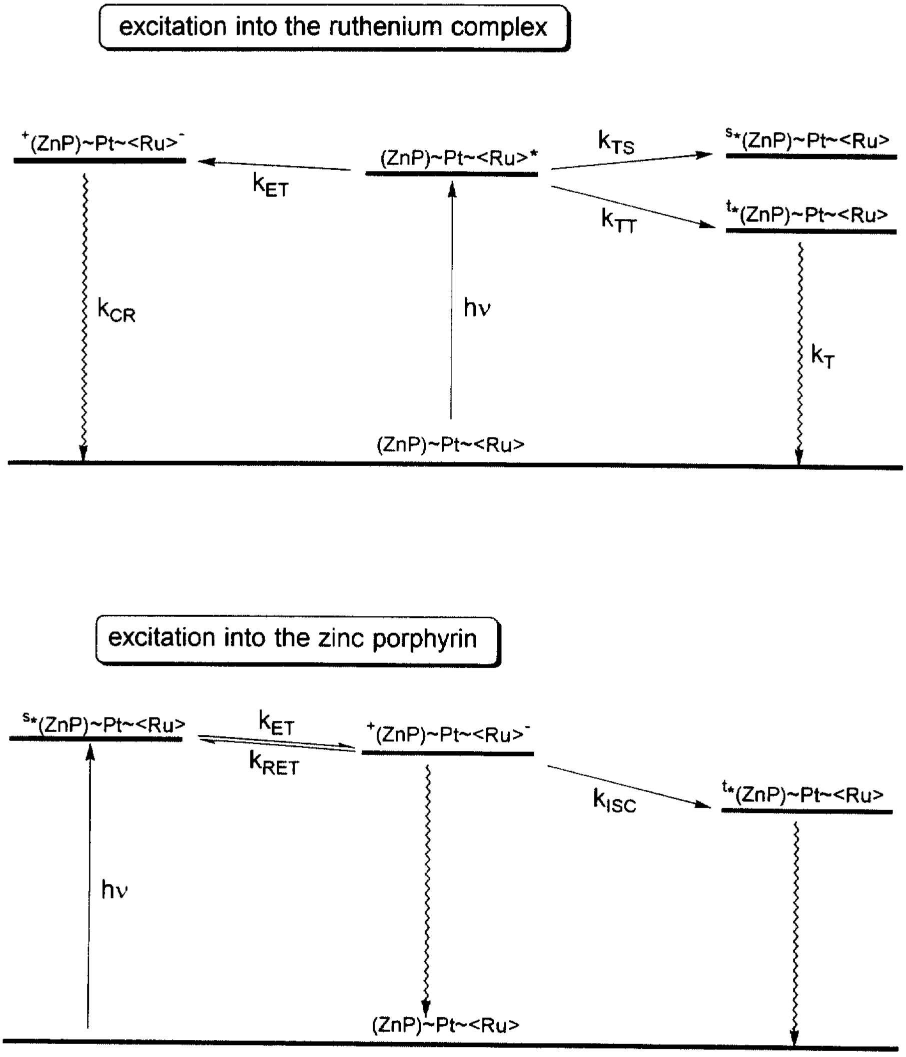

Fig. 18. Schematic representation of the important events that follow from selective illumination of the ZnP–Pt^{II}–Ru^{II} tripartite complex (**15**). Top: excitation into the terminal Ru^{II} complex gives rise to the corresponding excited triplet state. This species transfers energy to both singlet ($k_{TS}=1.7\times10^6$ s^{-1}) and triplet ($k_{TT}=3\times10^7$ s^{-1}) excited states of the porphyrin. A further deactivation route involves electron abstraction ($k_{ET}=3\times10^7$ s^{-1}) from ZnP to give a charge-separated state. This latter species undergoes charge recombination ($k_{TT}=9\times10^7$ s^{-1}) to restore the ground state. The triplet state of ZnP undergoes slow non-radiative decay ($k_T=1\times10^4$ s^{-1}) to the ground state. Bottom: excitation into ZnP causes immediate population of the excited singlet state localized on the porphyrin. This species undergoes reversible electron transfer ($k_{ET}=7.5\times10^8$ s^{-1}; $k_{RET}=6.0\times10^8$ s^{-1}) to form the charge-separated state. This latter species is sufficiently long-lived for intersystem crossing ($k_{ISC}=4\times10^7$ s^{-1}) to compete with charge recombination.

constant of ca. $2\times10^6\ s^{-1}$ and accounts for <5% of the overall photon balance. Triplet-to-triplet energy transfer to the adjacent ZnP, this process being spin-allowed, accounts for some 50% of the overall photon balance and occurs with a rate constant of ca. $3\times10^7\ s^{-1}$. However, an additional quenching process involves intramolecular electron transfer from ZnP to the triplet excited state of the ruthenium(II) *tris*(2,2′-bipyridyl) fragment. This reaction, for which the thermodynamic driving force is negligible ($\Delta G^\circ \approx 0$ eV), takes place with a rate constant of ca. $2.7\times10^7\ s^{-1}$. Charge recombination results in partial formation of the triplet excited state of the appended ZnP.

Direct illumination into the Q-bands localized on the ZnP results in the appearance of fluorescence characteristics of that porphyrin. The intensity of this emission is quenched relative to that measured for the appropriate reference compounds, while time-resolved fluorescence studies showed that the excited singlet state of the ZnP decays via dual-exponential kinetics. Consideration of the various energy levels allows us to conclude that the only viable quenching process for this system involves electron transfer from the excited singlet state of the ZnP to the neighboring ruthenium(II) *tris*(2,2′-bipyridyl) fragment. In this case, the dual-exponential decay profile indicates that light-induced electron transfer is reversible [70–72], enabling rate constants for the individual steps to be derived from the kinetic analysis (Fig. 18). The rate of forward electron transfer is kept slow by the negligible thermodynamic driving force ($\Delta G^\circ \approx 0$ eV) and by the relatively large separation distance over which the electron must tunnel.

It is interesting to consider the pathway for light-induced electron transfer in this system [73]. Transient absorption spectroscopic studies, together with the time-resolved emission experiments, indicate that illumination causes immediate formation of the first excited singlet state of the ZnP (Fig. 19). The promoted electron must tunnel through the connecting Pt^{II} *bis*-acetylide to the covalently bound 2,2′-bipyridyl ligand. Because of intramolecular charge transfer from the central Pt^{II} cation to this attached ligand, there will be a small thermodynamic driving force for the electron to migrate to one of the auxiliary 2,2′-bipyridyl ligands [22]. Thus, the redox equivalents become separated by ca. 28 Å. Charge recombination most likely also takes place by way of a cascade of electron transfers involving the LUMOs of the bridging organic framework. The rate constant for charge recombination is ca. $9\times10^7\ s^{-1}$, reflecting the long-range electron-transfer event and the large amount of energy that must be dissipated in the form of vibrational modes [74]. The latter is sufficient to push the charge-recombination process well into the Marcus inverted region [52].

Following direct excitation into the ruthenium(II) *tris*(2,2′-bipyridyl) fragment, it is most likely, at least on energetic grounds, that formation of the ultimate charge-separated state occurs by way of hole transfer (Fig. 20). Again, charge recombination will take place by way of a small cascade of electron-transfer events that results in partial formation of the triplet state of ZnP.

The rate of electron transfer from ZnP to the appended ruthenium(II) *tris*(2,2′-bipyridyl) fragment is relatively slow, regardless of which chromophore is illuminated. The two main reasons for the reluctance of the electron to tunnel between

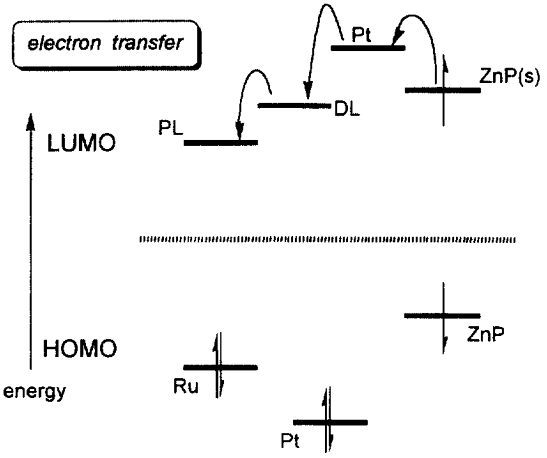

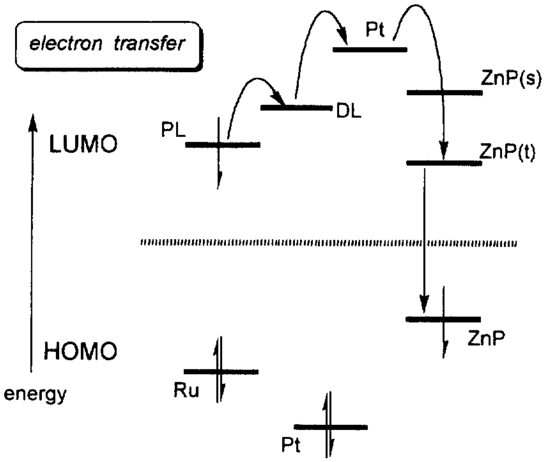

Fig. 19. Projected pathways for forward and reverse electron transfer in the ZnP–Pt^{II}–Ru^{II} tripartite complex (**15**) following selective excitation into ZnP. Both reactions are expected to occur via a cascade of electron-transfer steps involving intermediary (or virtual) reduction of Pt^{II}, the ditopic ligand (DL), and the parent ligand (PL). The two reactions take place through the LUMOs and, therefore, are designated as electron-transfer processes.

terminals are: (i) the negligible thermodynamic driving force for net electron transfer; and (ii) the high-energy barrier imposed by the central Pt^{II} *bis*-σ-acetylide. Both problems would disappear if a higher-energy excited state of reasonable lifetime could be accessed and, in fact, this is the case when illumination is made directly into the Soret band of ZnP. The Soret band corresponds to population of the second

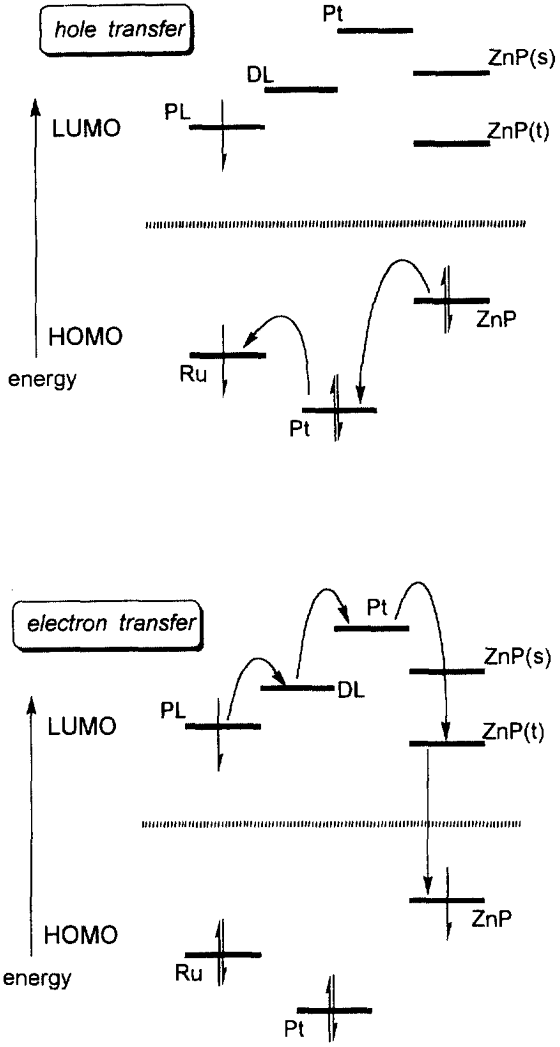

Fig. 20. Projected pathways for forward and reverse electron transfer in the ZnP–Pt^{II}–Ru^{II} tripartite complex (**15**) following selective excitation into the terminal Ru^{II} complex. Forward reaction is expected to proceed via hole transfer involving the respective HOMOs and forming Pt^{III} as a virtual intermediate. Charge recombination is expected to proceed by way of a cascade of electron-transfer steps involving the various LUMOs. This latter process results in partial population of the triplet excited state of ZnP.

excited singlet state and, according to the results of a transient absorption spectroscopic investigation, the lifetime of this upper-excited state is a few picoseconds. Illumination into this absorption band provides sufficient energy for the promoted electron to tunnel across to the ruthenium(II) *tris*(2,2′-bipyridyl) fragment since the thermodynamic driving force is now increased to ca. 0.9 eV. The electronic energy available to this upper-excited state ($\Delta E \approx 2.95$ eV) is sufficient to promote superexchange interactions through the bridging $\mathrm{Pt^{II}}$ *bis*-σ-acetylide.

This type of multicomponent system could become extremely important in future molecular-scale electronic devices because of its selectivity. The same intermediate state can be reached from three different starting points, each route taking a characteristic reaction time. Since individual precursor states are poorly connected, the system retains a memory and the time scale is determined by the color of the [monochromatic] excitation pulse. This system is considered to be among the most advanced in the field of photoelectronic devices.

8. The pyrene–Pt–Ru(bpy)$_3$ system

Direct attachment of pyrene to 2,2′-bipyridine (**16** in Fig. 16) via a single ethynylene bridge gives rise to a simple molecular dyad that forms a highly-fluorescent charge-transfer species in polar solvents [75]. According to detailed cyclic voltammetry studies, this species is generated by way of charge transfer from pyrene to the appended 2,2′-bipyridyl terminal. The charge-transfer species, which is clearly visible in the absorption spectrum, exhibits a Gaussian-shaped fluorescence band whose energy at the peak maximum increases steeply with decreasing polarity of the solvent. In non-polar solvents, such as CCl_4, local fluorescence from the π, π* states of the pyrene chromophore is seen. Upon coordination of a ruthenium(II) or osmium(II) organometallic fragment to the vacant 2,2′-bipyridine ligand, the charge-transfer emission is extinguished (complexes **26** and **27** in Fig. 21). This is because coordination to the metal center favors charge transfer to such an extent that illumination

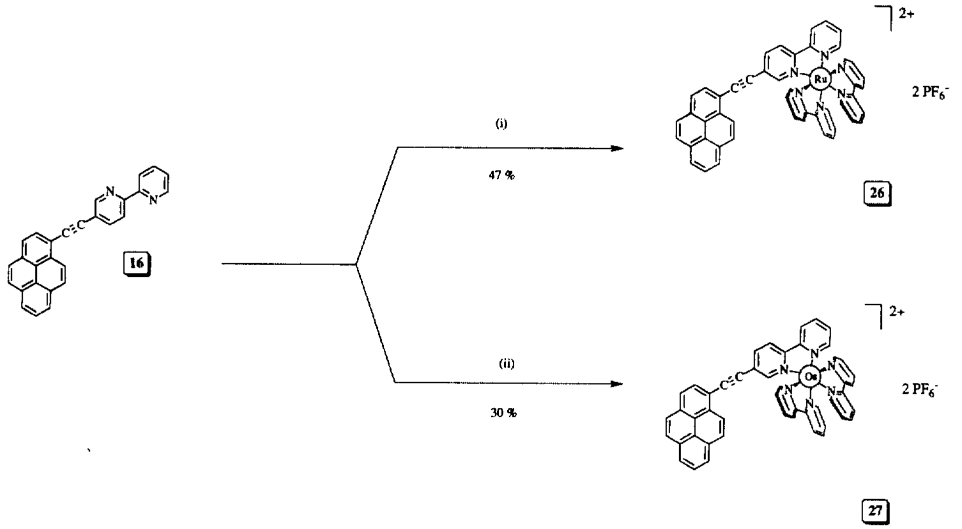

Fig. 21. Synthetic route used to prepare the mononuclear Ru(II) and Os(II) complexes (**26** and **27**): (i) 1 equiv. $[Ru(bpy)_2Cl_2] \cdot 2H_2O$, C_2H_5OH, 80 °C, 16 h; (ii) 1 equiv. $[Os(bpy)_2Cl_2]$, C_2H_5OH, 80 °C, 16 h.

into the pyrene chromophore is followed by immediate electron transfer to the complexed 2,2′-bipyridine. Charge recombination restores the original system on the time scale of a few hundred picoseconds. Thus, in these directly-attached molecular dyads, the terminals remain in very strong electronic communication such that both forward and reverse electron-transfer steps are fast.

For the ruthenium(II) *tris*(2,2′-bipyridyl)-based dyad (**22** in Fig. 16) [68], direct illumination into the MLCT absorption band associated with the metal complex does not give rise to appreciable luminescence characteristic of that metal complex. The triplet lifetime of the ruthenium(II) *tris*(2,2′-bipyridyl) unit was found to be very short, indicating that there exists an effective quenching pathway. This quenching can be attributed to intramolecular triplet energy transfer from the metal complex to the appended pyrene moiety. The triplet state of this latter chromophore is shifted to lower energy because of conjugation with the alkyne spacer [Fig. 22(a)]. However, the triplet energy of the pyrene unit remains above that of the corresponding osmium(II) *tris*(2,2′-bipyridyl) complex since luminescence from this species is readily detected following illumination into the MLCT absorption band.

Inserting a Pt^{II} *bis*-σ-acetylide between pyrene and 2,2′-bipyridyl units inhibits formation of the intramolecular charge-transfer complex and, following illumination into the pyrene absorption bands, local π, π^* fluorescence from the pyrene unit is seen. This finding is further testimony to the remarkable ability of the central Pt^{II} center to impose a high-energy barrier to through-bond electronic coupling. Upon coordination of ruthenium(II) or osmium(II) organometallic fragments to the vacant 2,2′-bipyridyl moiety in complexes **21** and **22** (Fig. 16), fluorescence from the pyrene unit is completely quenched. This is due to rapid Förster-type singlet-to-singlet energy transfer from pyrene to the MLCT band of the metal complex [Fig. 22(b)]. Thus, with the Pt^{II} *bis*-σ-acetylide bridged complexes, the terminal pyrene unit functions as a light-harvester and intramolecular electron transfer no longer takes place. This is a major change in reaction mechanism. It is important to note, however, that highly efficient energy transfer occurs in this system, unlike the case described previously for the Ru^{II}–Pt^{II}–Os^{II} mixed-metal system. This indicates that, by proper selection of the terminal units, the insulatory properties of the Pt^{II} *bis*-σ-acetylide can be overcome.

Direct illumination into the MLCT absorption bands associated with the terminal metal complex gives rise to very weak luminescence characteristic of the triplet state of the Ru^{II} analogue, whereas emission from the Os^{II} complex appears to be unquenched [76]. For the Ru^{II} complex, luminescence quenching is due to intramolecular triplet energy transfer to the pyrene unit. The rate constant for this energy-transfer process is $1.7 \times 10^8\ s^{-1}$ at room temperature. Because conjugation with the alkyne is hindered by the central Pt^{II} *bis*-σ-acetylide, the triplet energy of the pyrene unit remains well above that of the Os^{II} complex. Triplet energy transfer does not take place in this latter system and the triplet lifetime of the Os^{II} complex remains at ca. 75 ns [Fig. 22(a, b)].

The reason why intramolecular triplet energy transfer does not occur from the osmium(II) *tris*(2,2′-bipyridyl) complex to the appended pyrene is because the reaction is endothermic and unable to compete with the fast non-radiative deactiva-

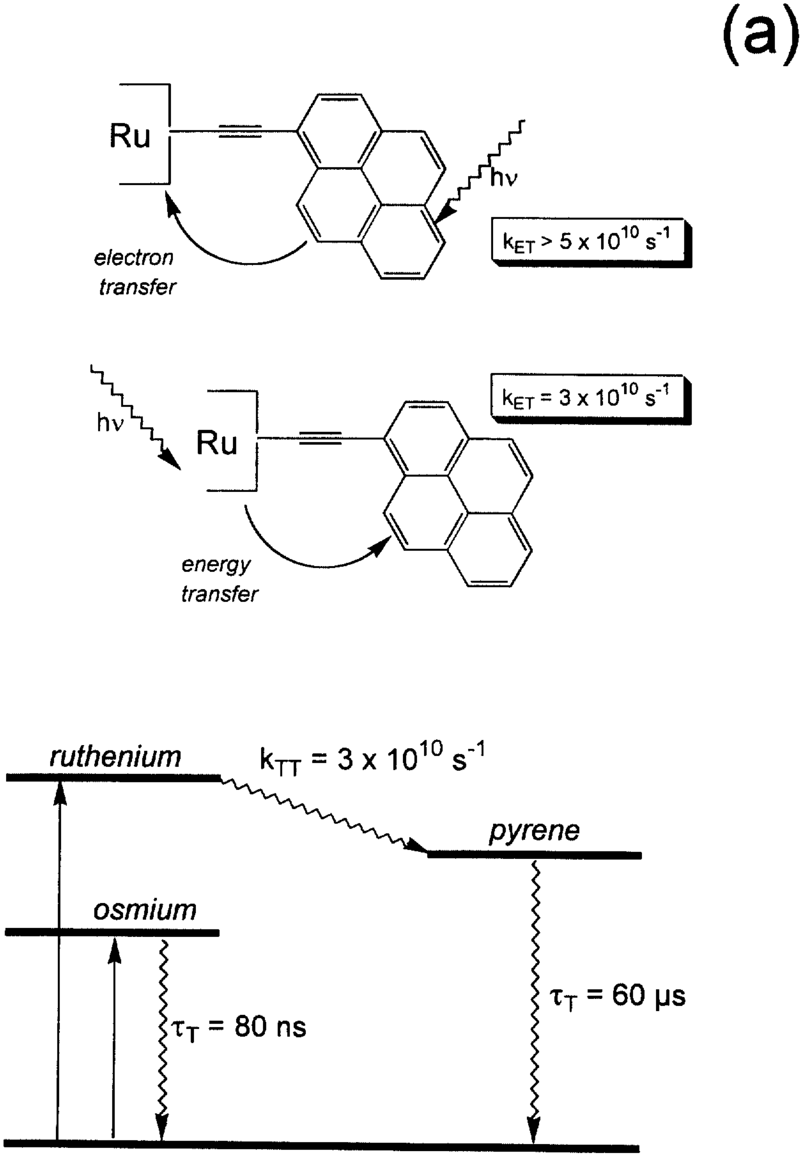

Fig. 22. Pictorial representation of the events that follow from selective illumination of the ethynylene-bridged pyrene–Ru^{II} *tris*(2,2′-bipyridyl) dyad (**26**) and the pyrene–Pt^{II}–Ru^{II} *tris*(2,2′-bipyridyl) conjugate (**22**). (a) Illumination into the pyrene chromophore causes rapid electron transfer to the appended metal complex, whereas illumination into the Ru^{II} *tris*(2,2′-bipyridyl) complex is followed by extremely fast triplet energy transfer to pyrene. For the corresponding pyrene–Os^{II} *tris*(2,2′-bipyridyl) dyad (**27**), triplet energy transfer to the pyrene unit does not occur because of the unfavorable energy level positioning. (b) Irradiation into the pyrene chromophore causes rapid singlet energy transfer to the appended metal complex, whereas illumination into the Ru^{II} *tris*(2,2′-bipyridyl) complex is followed by slower triplet energy transfer to pyrene. For the corresponding pyrene–Pt^{II}–Os^{II} *tris*(2,2′-bipyridyl) tripartite complex (**21**) the triplet state of the metal complex is located at low energy and does not transfer energy to pyrene.

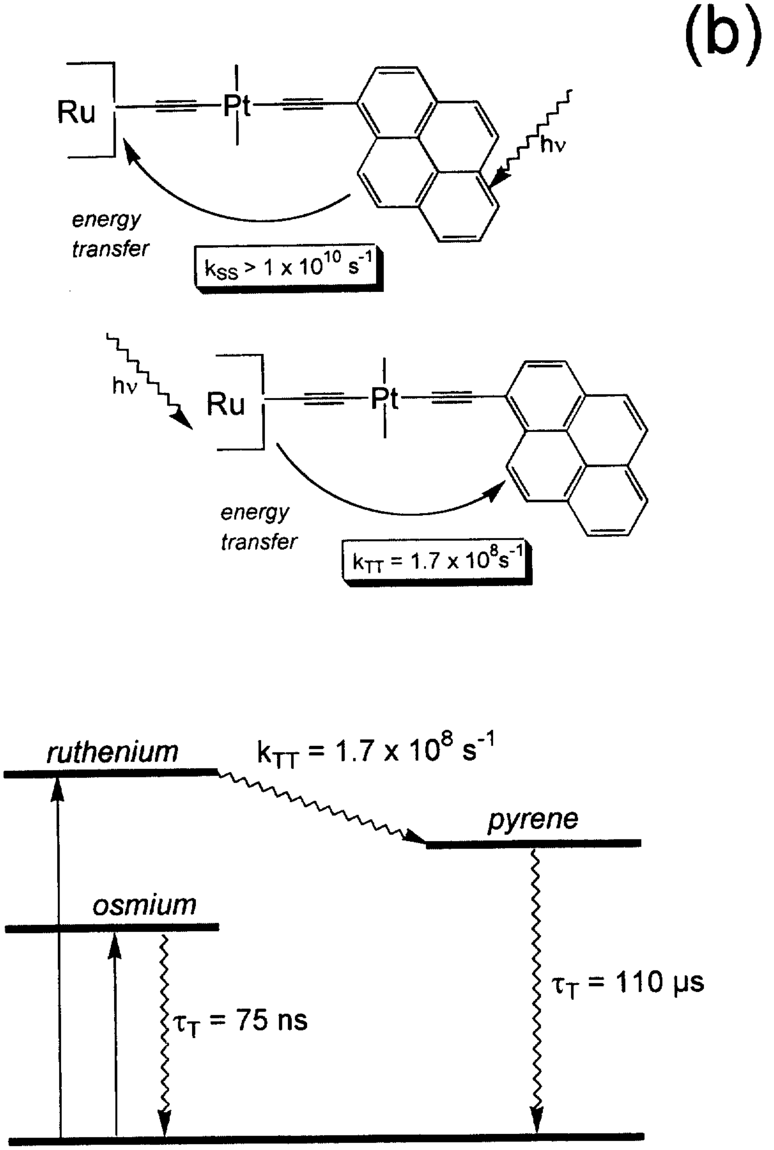

Fig. 22. (*continued*)

tion of the donor triplet state. A more interesting question, however, is why does triplet energy transfer from the ruthenium(II) *tris*(2,2′-bipyridyl) unit take place to pyrene at a reasonable rate when this process is inefficient in the analogous *trans*-RuPtOs mixed-metal complex [21,22]. This becomes a particularly intriguing mechanistic puzzle when it is recalled that the Förster-type overlap integral for triplet energy transfer to pyrene will be substantially smaller than that for transfer to an osmium(II) *tris*(2,2′-bipyridyl) unit because of the less favorable absorption spectral profile. Also, the center-to-center separations remain comparable for the two systems. Clearly, triplet energy transfer does not take place via dipole–dipole interactions but must involve through-bond electron exchange [46,50]. In this case, the edge-to-edge separation distance is much smaller with pyrene because with an osmium(II) fragment as the energy acceptor the electron has to tunnel across to one of the parent ligands, thereby greatly increasing the distance for electron transfer. It is also reasonable to expect that the energetics of the Pt^{II} *bis*-σ-acetylide bridge differ markedly in the two cases. For the Ru^{II}–Pt^{II}–Os^{II} mixed-metal dyad, the Pt^{II} center donates charge to both appended 2,2-bipyridyl units whereas, according to cyclic voltammetry, pyrene donates charge to the central Pt^{II} core. In the latter case, there will be increased electron density at the Pt^{II} center but in the Ru^{II}–Pt^{II}–Os^{II} mixed-metal dyad the central organometallic unit will be electron deficient.

Again, it becomes clear that proper design of the system avoids the insulatory behavior of the Pt^{II} *bis*-σ-acetylide bridge so that efficient intramolecular energy transfer becomes possible. This means that the valuable design elements inherent to this organometallic building block are not wasted. The light-harvesting features shown by the terminal pyrene unit open up new possibilities, especially with regard to the construction of larger arrays comprising numerous discrete units.

9. Changing the energy of the bridging unit

The above discussion has illustrated the point that the electronic properties of a polyacetylenic bridge can be modulated over a wide range by incorporating additional units into the unsaturated backbone. Since the polyacetylene itself is extremely effective at promoting long-range electronic coupling between terminals [1–4], the primary function of these adventitious units is to decrease the magnitude of electronic communication along the molecular axis. It is necessary that the insulatory properties of such components can be tuned to match that of the photoactive terminal so as to introduce unidirectionality of electron flow. In this way, the properties of bridge and terminal can be optimized for specific processes and, in turn, this permits the introduction of selectivity into the overall system. It is only by being selective for particular processes that these molecular systems will display useful electronic properties. Having demonstrated that it is possible to severely disrupt electron propagation along the molecular-scale wire, we now seek to provide a more subtle means for controlling the energetics of the bridge.

One simple way by which to modulate the electronic coupling properties of a polyacetylenic bridge is to insert polycyclic hydrocarbons at predetermined positions along the wire [77]. Our earlier attempts in this direction positioned phenyl rings at the connection point between coordinating oligopyridine ligand and the acetylene [42]. This approach is flawed because of the inherent difficulty in achieving proper orbital overlap between adjacent phenyl rings [7–11]. Such problems are removed simply by ensuring that there is at least one ethynylene group between the phenyl rings. An obvious advantage of this approach is that the energy of the bridging unit

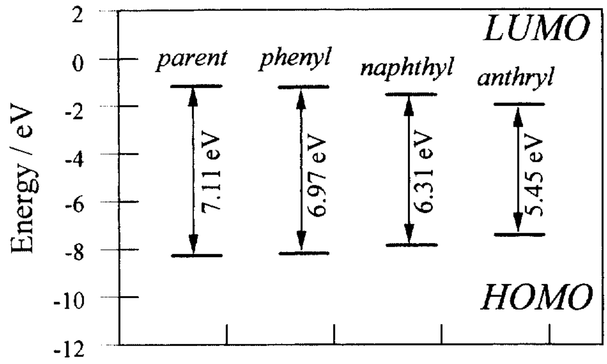

Fig. 23. Calculated LUMO and HOMO energy levels for a series of 1,4-diphenylbutadiynes containing a central relay. The nature of the relay (1,4-phenyl, 1,4-naphthyl, or 9,10-anthryl) affects the energy of both the LUMO and HOMO and there is a progressive decrease in energy gap with increasing size and conjugation of the relay.

can be controlled by the nature of the polycycle. This situation is illustrated by the results of a series of molecular orbital calculations made using PM3 parameters. Thus, the energy of both HOMOs and LUMOs resident on the bridge is determined by the degree of conjugation of the interspersed polycycle (Fig. 23). More refined modulation of the energetics is achieved by varying the site of attachment of the acetylene groups on the naphthalene moiety (Fig. 24). A second important feature of this approach is that the solubility of the emerging supermolecule can be improved

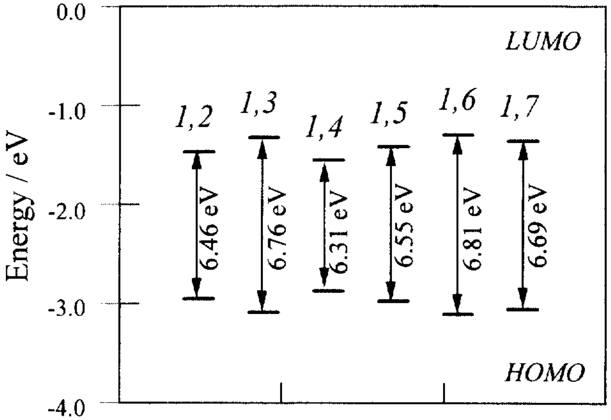

Fig. 24. Calculated LUMO and HOMO energy levels for a series of diphenylbutadiynes containing a central naphthyl residue. It is seen that the site at which the ethynylene units are attached to the naphthalene relay affects the energy of both LUMO and HOMO, with the 1,4-linkage giving the lowest energy gap. These calculations suggest that the ability of the bridge to promote through-bond electronic coupling might depend on the positions at which the bridge is connected to the relay. Note, 5 eV has been added to the position of the HOMO (but not the quoted energy gap) to clarify presentation.

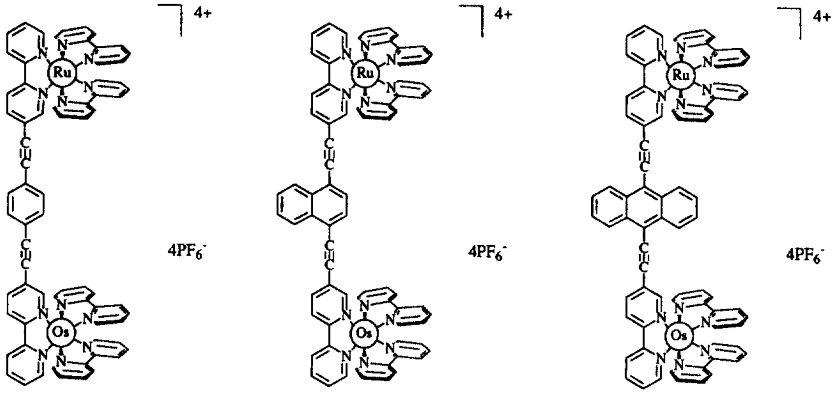

28 **29** **30**

Fig. 25. Schematic representation of the RuOs mixed-metal complexes (**28**–**30**) assembled around a central mono- or polycyclic relay.

by attachment of suitable functionalities to the polycycle. The same methodology can be used to provide the necessary functions for inclusion into organized media.

When used in this way, these adventitious groups built into the polyacetylenic wire operate as electronic relays. They provide a modest barrier to electron flow but, with the correct choice of reactants, electrons can tunnel through the barrier at a reasonable rate. This is in marked contrast to the insulating effect of Pt^{II} *bis*-σ-acetylide complexes [22]. Whether or not the relay functions as a real intermediate in the overall process depends upon the relative energetics of terminal and relay and, therefore, is system dependent. Because short-range interactions are involved, rates of electron propagation along the wire tend to be very fast and unidirectional.

We can illustrate the power of this approach by considering the triplet energy transfer processes that take place in the mixed-metal complexes **28**–**30** shown in Fig. 25. Here, ruthenium(II) *tris*(2,2′-bipyridyl) and osmium(II) *tris*(2,2′-bipyridyl) units are appended at either end of a 1,4-diethynylated polycycle whose size is varied [76]. Illumination into the terminal ruthenium(II) *tris*(2,2′-bipyridyl) unit generates the triplet excited state of that species, for which the inherent lifetime in deoxygenated acetonitrile at 20 °C is ca. 1 μs. The average metal-to-metal separation is ca. 18.3 Å in each case. For the phenyl-bridged Ru–Os complex, the triplet lifetime of the Ru moiety is only ca. 1.4 ns. This quenching process is due to intramolecular triplet energy transfer to the appended osmium(II) *tris*(2,2′-bipyridyl) complex, the triplet state of this latter species remaining unquenched with a lifetime of ca. 80 ns. Thus, electron exchange takes place across the interspersed phenyl ring and is quantitative at room temperature (Fig. 26).

In the naphthyl-bridged Ru–Os system, luminescence from the terminal ruthenium(II) *tris*(2,2′-bipyridyl) fragment cannot be detected at either 20 °C in fluid solution or at 77 K in an ethanol glass. The lifetime of this triplet state was

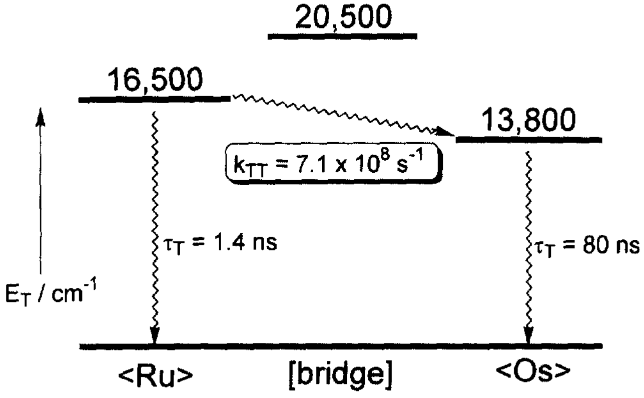

Fig. 26. Pictorial representation of intramolecular triplet energy transfer in the phenyl-bridged Ru^{II}–Os^{II} mixed-metal dyad (**28**). The energy level of each terminal metal complex is taken from luminescence spectra recorded at 20 °C while the energy level for the bridge is taken as being that of the ditopic ligand measured at 77 K. Energy levels are quoted in units of cm^{-1}.

measured by transient absorption spectroscopy to be ca. 85 ps, such that intramolecular triplet energy transfer is extremely fast in this case. Energy transfer occurs to the central naphthalene residue rather than directly to the terminal osmium(II) *tris*(2,2′-bipyridyl) fragment. However, the energy of the triplet state localized on this naphthalene residue is slightly higher than the triplet energy of the corresponding osmium(II) *tris*(2,2′-bipyridyl) fragment so that these two triplets are in thermal equilibrium at room temperature. The triplet lifetime of the osmium(II) *tris*(2,2′-bipyridyl) complex is relatively short (Fig. 27). It should be noted that the two-step

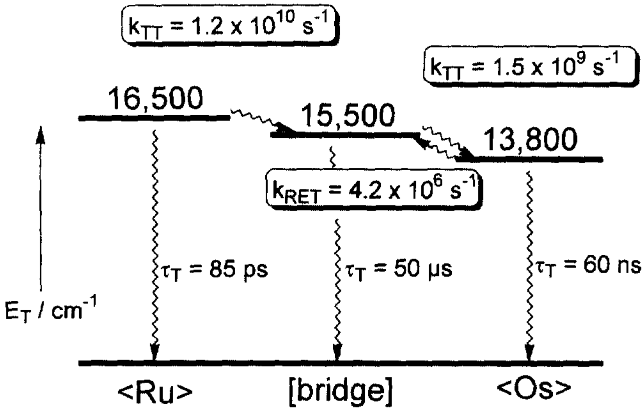

Fig. 27. Pictorial representation of intramolecular triplet energy transfer in the naphthyl-bridged Ru^{II}–Os^{II} mixed-metal dyad (**29**). The energy level of the Ru^{II} complex is assumed to be the same as that in Fig. 26, that of the Os^{II} complex is taken from the luminescence spectrum recorded at 20 °C, while that of the bridge is taken from luminescence spectra recorded at 77 K for the mononuclear complexes. Energy levels are quoted in units of cm^{-1}.

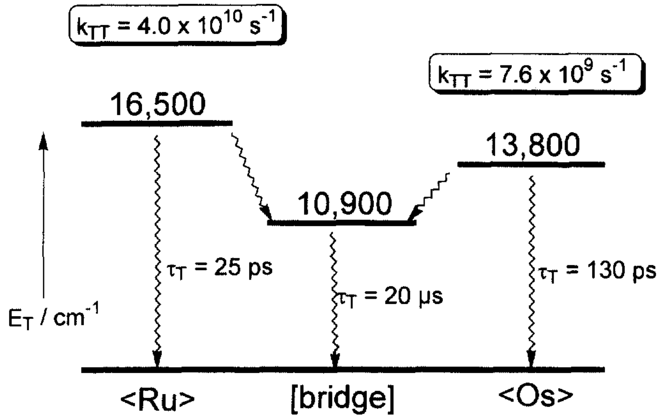

Fig. 28. Pictorial representation of intramolecular triplet energy transfer in the anthryl-bridged Ru^{II}–Os^{II} mixed-metal dyad (**30**). The energy level of each terminal metal complex is assumed to be the same as those given in Fig. 26, while that of the bridge is taken from luminescence spectra recorded at 77 K. Energy levels are quoted in units of cm^{-1}.

mechanism provides for rapid and quantitative energy transfer along the molecular axis.

The lifetime of the triplet state localized on the terminal ruthenium(II) *tris*(2,2′-bipyridyl) unit in the anthryl-bridged mixed-metal system is ca. 25 ps. Quenching is due to rapid energy transfer to the bridging anthracene residue [78–80], the triplet state of which is situated at very low energy (Fig. 28). Since the energy gap between the triplets localized on ruthenium(II) *tris*(2,2′-bipyridyl) unit and bridge is now substantially increased, the rate of energy transfer occurs close to the apex of a Marcus rate vs. energy-gap profile. Triplet energy transfer also takes place from the terminal osmium(II) *tris*(2,2′-bipyridyl) unit to the bridging anthracene residue.

It can be seen from these investigations that the energy of the bridging unit has a profound effect on both rate and pathway of intramolecular energy transfer. Decreasing the energy of the bridging triplet causes its direct participation in the energy-transfer sequence until, as in the case of anthracene, the bridge becomes a trap. In such a situation the photonic energy initially localized on either terminal complex is lost to a low-energy sink. The optimum bridging unit is somewhere between phenyl and naphthyl rings, where the rate of energy transfer will be very fast but sequential and irreversible. This realization indicates the particular importance of being able to insert tunable relays into the bridge.

10. Inclusion of additional coordination sites

So far we have described examples of transition metal complexes in which the same oligopyridine ligand is attached at opposite ends of a short bridge [1–4]. In such cases, the bridge is actually a ditopic ligand and the only way to achieve an energy gradient along the molecular axis is to coordinate disparate cations at vacant terminals. This approach is quite satisfactory for the introduction of a large energy gradient but a more subtle methodology is needed if one has to generate a shallow gradient covering numerous receptors. This is the only way to achieve a cascade of electron-transfer events without wasting too much of the available photonic energy [81–83]. We now consider if such a system can be engineered by including slightly different coordination sites into the bridge. In effect, this requires access to asymmetrical ditopic ligands capable of selective complexation and this is a difficult feat to realize.

This effect is illustrated in Fig. 29, where a hybrid bpy/terpy ligand [84] was allowed to react under classical conditions with either a "Ru(bpy)$_2$" or a "Ru(terpy)" metallo-precursor. In the case of Ru(bpy)$_2$, the hybrid ligand is selectively complexed at the bpy site, giving rise to a unique product possessing the required ruthenium(II) *tris*(2,2′-bipyridyl) fragment. Again, in the case of Ru(terpy) only the bpy site is complexed but now an unsuitable complex is generated.

In order to avoid such synthetic anomalies, we have developed an alternative strategy based on the use of functionalized metallo-synthons bearing one or more

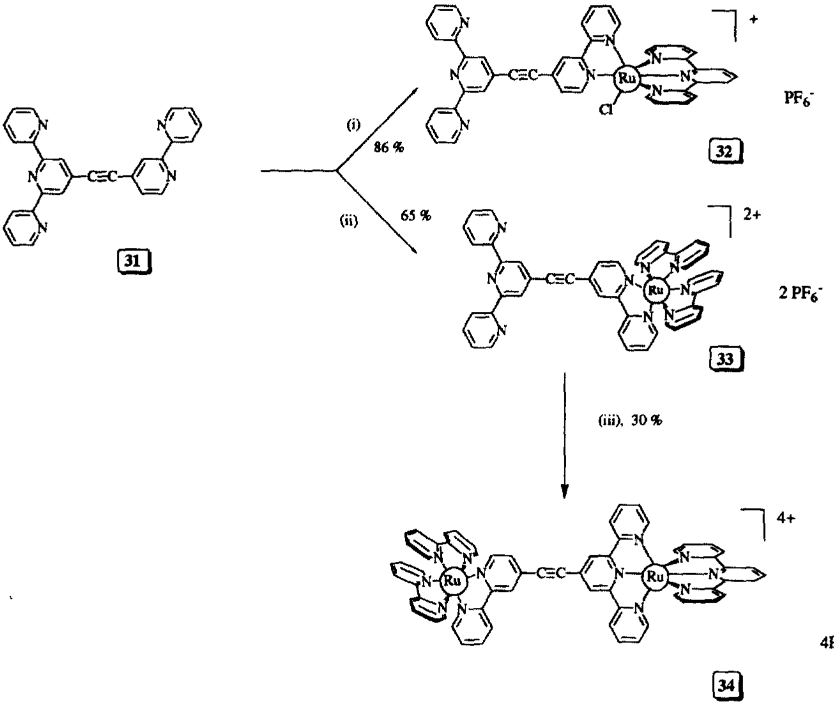

Fig. 29. Illustration of the complexation processes that occurs with the hybrid ligand (**31**). Reaction with an incoming Ru(II) metallo-fragment takes place at the vacant 2,2′-bipyridine site (**32**, **33**), apparently by-passing the nearby 2,2′:6′,2″-terpyridine ligand: (i) 1 equiv. [Ru(terpy)(S)$_3$]$^{2+}$, S=CH$_3$OH, CH$_3$OH, 80 °C, 5 days; (ii) 1 equiv. [Ru(bpy)$_2$Cl$_2$]·2H$_2$O, 80 °C, 24 h; (iii) 1 equiv. [Ru(terpy)(S)$_3$]$^{2+}$, in S=CH$_3$OH, in CH$_3$OH, 80 °C, 19 h.

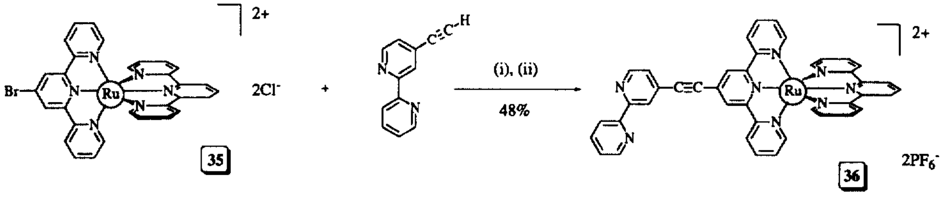

Fig. 30. Synthetic strategy used to gain access to the new binuclear Ru(II) hybrid complex **36**. (i) [Pd^0(PPh$_3$)$_4$] 6 mol%, CH$_3$CN/C$_6$H$_6$, (^{i}Pr$_2$)NH, 80 °C, 15 h; (ii) anion metathesis.

ethynyl or pseudo-halide groups in conjunction with non-complexed oligopyridino building blocks in Sonogashira-type cross-coupling reactions [58]. The synthetic protocol is illustrated in Fig. 30, where preparation of complex **36** is achieved by a cross-coupling reaction between 4-ethynylene-2,2′-bipyridine and the metallo-synthon **35**. Such coupling reactions operate smoothly in the presence of catalytic amounts of Pd(0). In fact, this convergent strategy turns out to be valid for the synthesis of many related hybrid complexes that could not be prepared by the classical method.

The new hydrid complex containing terminal ruthenium *tris*(2,2′-bipyridyl) and ruthenium(II) *bis*-terpyridyl units linked via an ethynylene spacer (**34** in Fig. 29) is particularly interesting [85]. The absorption spectrum shows a very clean set of transitions with the maximum for the MLCT band centered at 506 nm. It is not possible, however, to resolve the MLCT region into bands associated with the individual terminal complexes [Fig. 31(a)]. Luminescence is readily detected following excitation into the MLCT band and, in acetonitrile solution at 20 °C, the maximum is located at 705 nm [Fig. 31(b)]. This emission decays with a single exponential lifetime of 840 μs in deoxygenated solution. Even so, the luminescence spectrum can be deconstructed into two overlapping bands that correspond extremely well to the spectra recorded for the corresponding mononuclear Ru^{II} complexes [Fig. 31(b)]. We might consider that, at least at first glance, the triplet manifold of this hybrid complex consists of the two individual triplets in thermal equilibrium. This idea is fully supported by the excitation spectrum recorded for the hybrid complex.

A second example of the versatility of this synthetic method is illustrated in Fig. 32, showing preparation of the dinuclear complexes **37** and **38** starting from the metallo-synthon **35**. A special situation exists when, as in the case of **37**, the spacer function itself is equipped with vacant coordination sites [86]. This permits the energetics of the bridge to be controlled by binding secondary cations at the relay. Rather than intersperse the metal fragment directly into the polyacetylenic bridge, we can consider the case in which selected cations are bound outside the wire at the vacant coordination site. In this way, secondary coordination might be expected to influence the overall properties of the molecular system.

We can illustrate this strategy by considering the luminescence properties of the binuclear Ru^{II} *bis*-(2,2′:6,2″-terpyridyl) complex bridged with a *bis*-ethynylated 2,2′-bipyridyl spacer function (**37**). This complex emits weakly in deoxygenated methanol

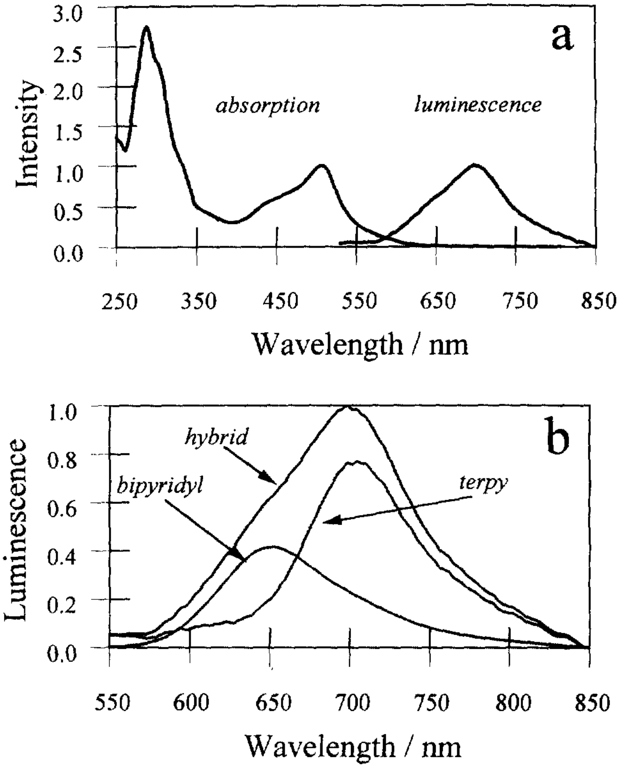

Fig. 31. (a) Absorption and emission spectra recorded for the binuclear Ru^{II} hybrid complex **34** in deoxygenated acetonitrile at 20 °C. (b) Deconstruction of the emission spectrum into components associated with the bipyridyl- and terpyridyl-based mononuclear complexes. This deconstruction procedure gives a good representation of the spectrum recorded for the hybrid complex.

solution at 20 °C with a maximum at 685 nm (Fig. 33) and a lifetime of 100 ns. Since no such luminescence can be detected for the reference Ru(terpy)$_2^{2+}$ complex, it is apparent that the promoted electron resides in a slightly extended π^* orbital localized on the ditopic ligand. This lowers the energy of the MLCT triplet excited state and, because there is less interaction with higher-energy excited states, increases the triplet lifetime with respect to the parent complex. Protonation of the interspersed bipyridyl function causes a slight increase in emission yield (Fig. 33) and the triplet lifetime increases to 115 ns. There is a 5 nm red-shift to the luminescence maximum, suggesting that protonation lowers the energy of the bridge [87]. Even so, electrostatic repulsion between adjacent protonated pyridine rings prevents the bipyridyl unit adopting a favorable geometry for effective electronic coupling. Complexation of the vacant bipyridyl function with Zn^{II} cations causes more significant modification of the photophysical properties (Fig. 33). In this case, the emission yield doubles, the triplet lifetime increases to 210 ns, and there is a further 15 nm red-shift to the emission maximum. These changes are considered to reflect the increased level of

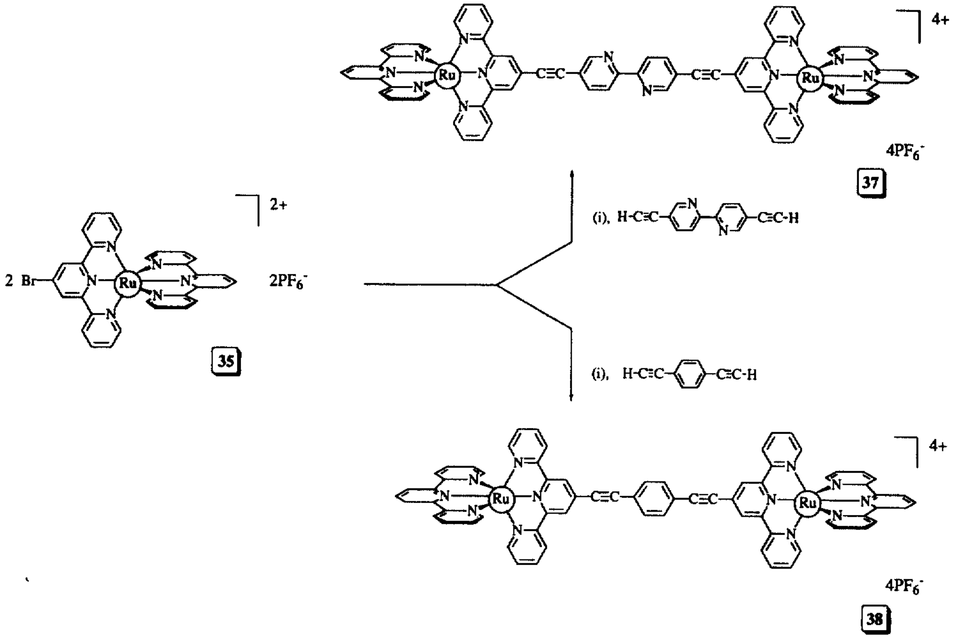

Fig. 32. Synthetic approach used to prepare the binuclear Ru(II) terpyridyl complexes having an aryl hydrocarbon positioned at the center of the ditopic ligand. Reaction utilizes a metallo-synthon (**35**) in the coupling reaction: (i) [Pd^{II}(PPh$_3$)$_2$Cl$_2$] 6 mol%, CH$_3$CN/C$_6$H$_6$, (^{i}Pr$_2$)NH, 25 °C, 6 days.

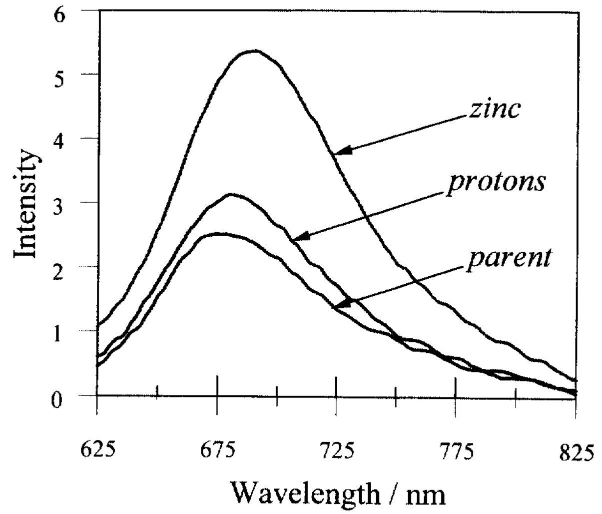

Fig. 33. Luminescence spectra recorded in deoxygenated acetonitrile for the bipyridyl-bridged binuclear Ru^{II} complex **37** (parent). Protonation of the interspersed bipyridyl unit (protons) causes a small red-shift and enhancement in luminescence, while complexation with zinc(II) cations (zinc) gives rise to a more substantial red-shift and enhancement.

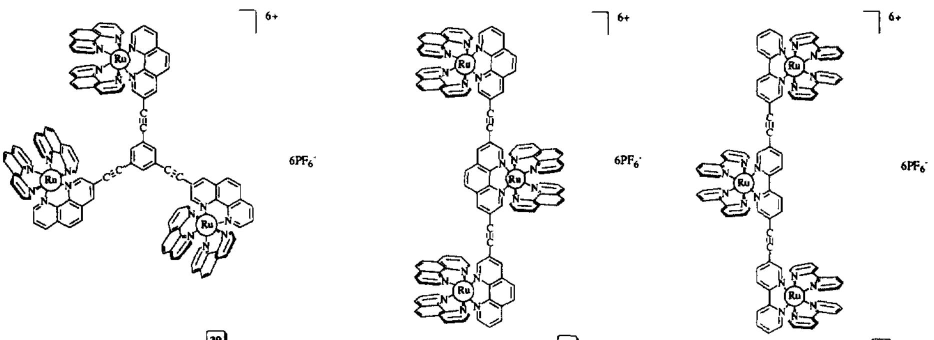

39 **40** **41**

Fig. 34. Structures of the various trinuclear Ru(II) complexes.

electronic coupling across the bipyridyl unit due to the adoption of a coplanar geometry upon complexation. Studies made with a water-soluble form of **37** in Fig. 32 confirm these findings and allow quantitative evaluation of both p*K* and complexation constant.

This synthetic approach is readily amenable for the construction of trinuclear and higher-order complexes by coordination of the same organometallic fragment to different binding sites along the molecular axis [88]. The trinuclear systems (**41** in Fig. 34) are interesting as simple models of a light-harvesting complex since there is a small energy gradient from peripheral to central metal complexes. In fact, we are now in a position to consider the triplet energy transfer processes that take place in longer molecular arrays since we know all the necessary rate constants. Thus, the rates of energy migration between adjacent Ru^{II} or Os^{II} units of identical structure have been measured for symmetrical binuclear complexes (Fig. 35). Similarly, rates of forward and reverse energy transfer have been measured for the corresponding trinuclear complexes [1]. Once these rates have been shown to apply to the linear tetranuclear complex (Fig. 35) it becomes possible to construct a simple kinetic scheme that could be used to model energy diffusion in much larger arrays. Related trinuclear phenanthroline-based complexes have recently been prepared using palladium-mediated, cross-coupling reactions (Fig. 34) [89,90].

11. Extending the bridge by subsequent complexation

Earlier studies [42] have shown that short polyacetylenic bridges provide for extended electron delocalization over the ditopic ligand within the triplet manifold of symmetrical binuclear metal oligopyridine complexes. Such electron delocalization over an extended π^* orbital causes, among other features, a decrease in the energy of the triplet state due to increased conjugation [46]. The extent of internal electron delocalization depends markedly on the energy gradient along the molecular axis, as can clearly be seen from the following comparison. Thus, the emission maximum for ruthenium(II) *bis*-terpyridyl, as estimated from luminescence spectral curve

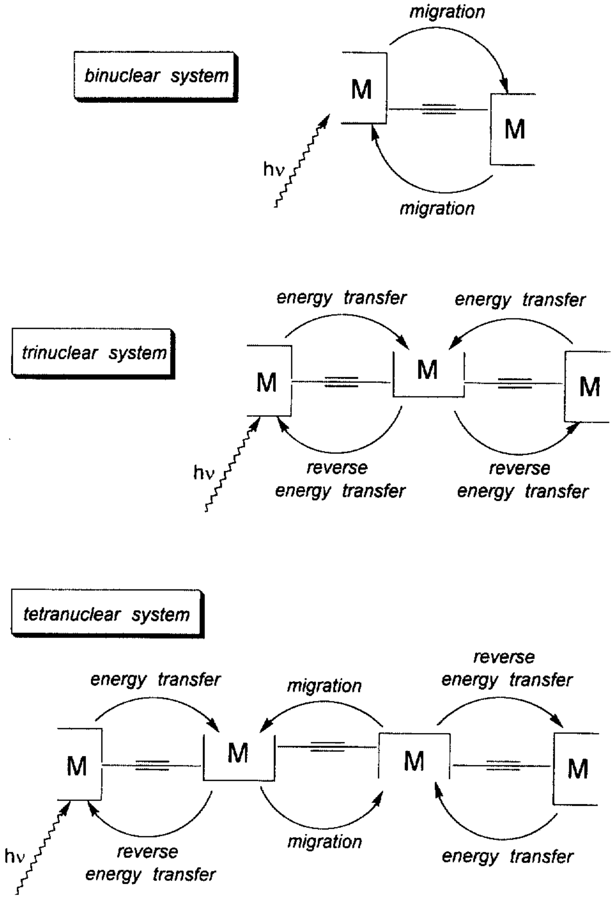

Fig. 35. Pictorial representation of the triplet energy-transfer processes that can take place in polynuclear metal oligopyridine complexes. In the symmetrical binuclear complex, triplet energy migration occurs on the nanosecond time scale so that an absorbed photon effectively shuttles between the two terminals. A small energy gradient causes the central metal complex to possess a lower triplet energy than the terminal complexes in the trinuclear complex. Thus, photons absorbed by either terminal are transferred to the central unit but, since the energy gap is small, reverse energy transfer can occur to establish a thermal equilibrium of triplet states. All three reactions (migration, transfer, and reverse transfer) can take place in higher-order polynuclear complexes. Knowledge of the various rate constants allows estimation of the probability of finding the photon at any given site, regardless of which unit absorbed the photon.

analysis at 77 K, is 610 nm [42]. Attaching a vacant terpyridyl ligand via a single ethynylene group to one of the coordinated terpyridine ligands allows extension of the π* orbital and pushes the emission maximum to 675 nm. Binding an identical ruthenium(II) organometallic fragment to this vacant terpyridyl ligand, giving the symmetrical complex, causes a further shift in emission maximum to 700 nm. Instead of binding the second ruthenium(II) center it is possible to coordinate other cations that do not function as electron or energy acceptors, such as zinc(II) or protons

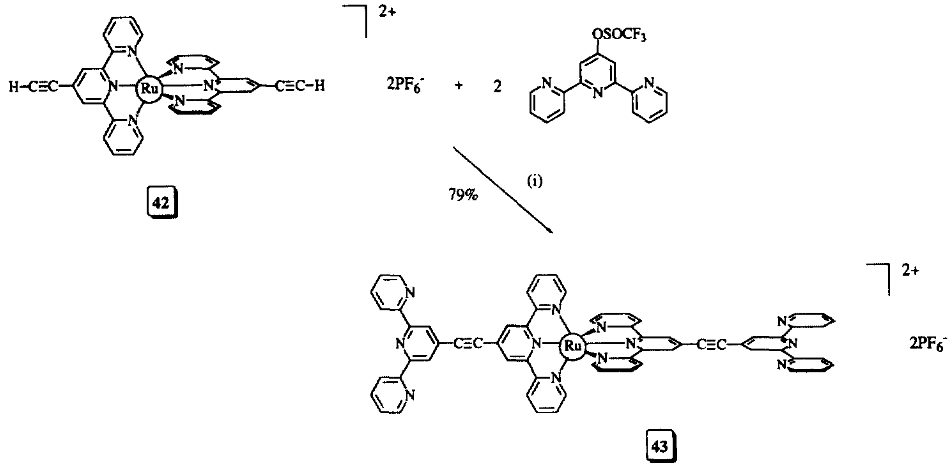

Fig. 36. Illustration of the multiple coupling reactions available with the difunctionalized metallo-synthon **42**: (i) [Pd^0(PPh$_3$)$_4$] 6 mol%, CH$_3$CN/C$_6$H$_6$, (^{i}Pr$_2$)NH, 80 °C, 4 days.

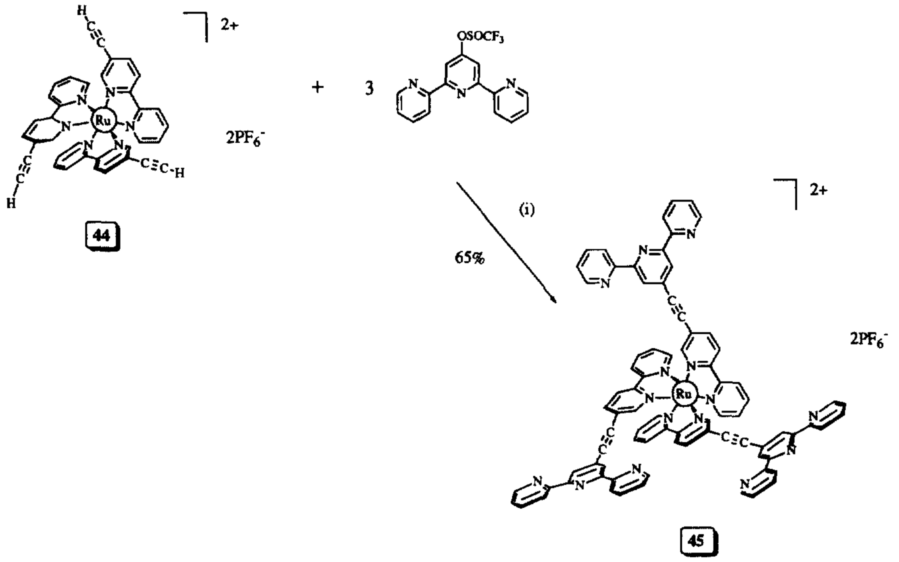

Fig. 37. Examples of cross-coupling reactions available to the trifunctionalized metallo-synthon **44**: (i) [Pd^0(PPh$_3$)$_4$] 6 mol%, CH$_3$CN/C$_6$H$_6$, (^{i}Pr$_2$)NH, 80 °C, 24 h.

[41,87]. In this case, the degree of electron delocalization depends on how closely the energy of each terminal unit matches the other; the optimum delocalization occurring when the terminals are isoelectronic.

The case with coordination of zinc(II) cations is especially interesting because the end of the two terminals is not too disparate in energy. Thus, the emission

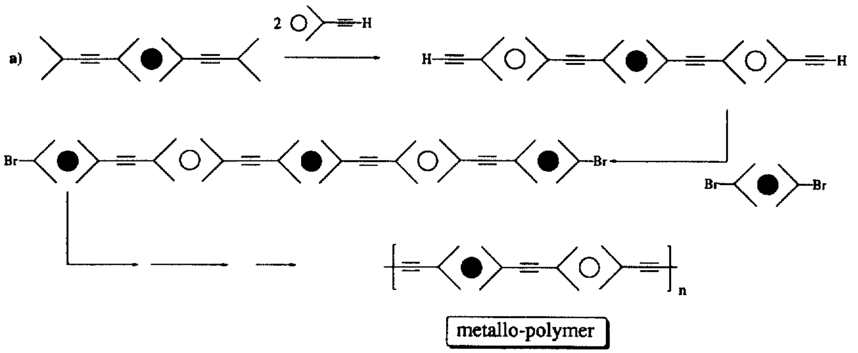

Fig. 38. Extension of the synthetic strategy to generate (a) metallo-polymers or (b) metallo-dendrimers.

maximum recorded for the zinc(II) complex is at 675 nm and lies between that of the symmetrical binuclear complex and the mononuclear complex [41]. This means that zinc(II) cations can be used to extend the molecular length by acting as a coordination site for assembling two identical mononuclear complexes into a linear trinuclear system. It is important to realize that the alkyne substituent renders that particular ligand more easily reduced than the coordinated auxiliary ligand such that charge injection will take place preferentially to the substituted ligand under illumination. The promoted electron resides in an extended π* orbital that encompasses at least a substantial part of the bridge. When different metal complexes are positioned at either end of the molecular axis there is only a small barrier to through-bond electron or hole transfer. Since the terminal cations are now separated by ca. 28 Å it is clear that this approach, although synthetically challenging, offers many possibilities for building linear supermolecules that retain interesting photo properties.

12. Varying the shape of the array

The generality of our synthetic protocol is shown in Figs. 36 and 37. Here, double or triple cross-coupling reactions between terpy-triflate and a Ru-synthon possessing either two alkyne-functionalized terpy ligands (in **42**) or three alkynylated bipy ligands (in **44**) were used to prepare complexes **43** and **45**, respectively, in high yield [58]. These latter complexes bear vacant coordination sites and have been designed, respectively, for the subsequent assembly of metallo-polymers [Fig. 38(a)] or metallo-dendrimers [Fig. 38(b)]. The free coordination sites present in complexes **43** and **45** (Figs. 36 and 37), in principle, could be selectively coordinated with appropriate metal fragments that possess the necessary functionality to continue the synthetic sequence and/or to change the geometry. Further iteration of complexation/cross-coupling reactions provides the means by which to extend the array and to incorporate desired metallo-centers at predetermined sites. The future of this field will also include the preparation of soluble σ-alkynyl rigid-rod polymers bearing chromo-

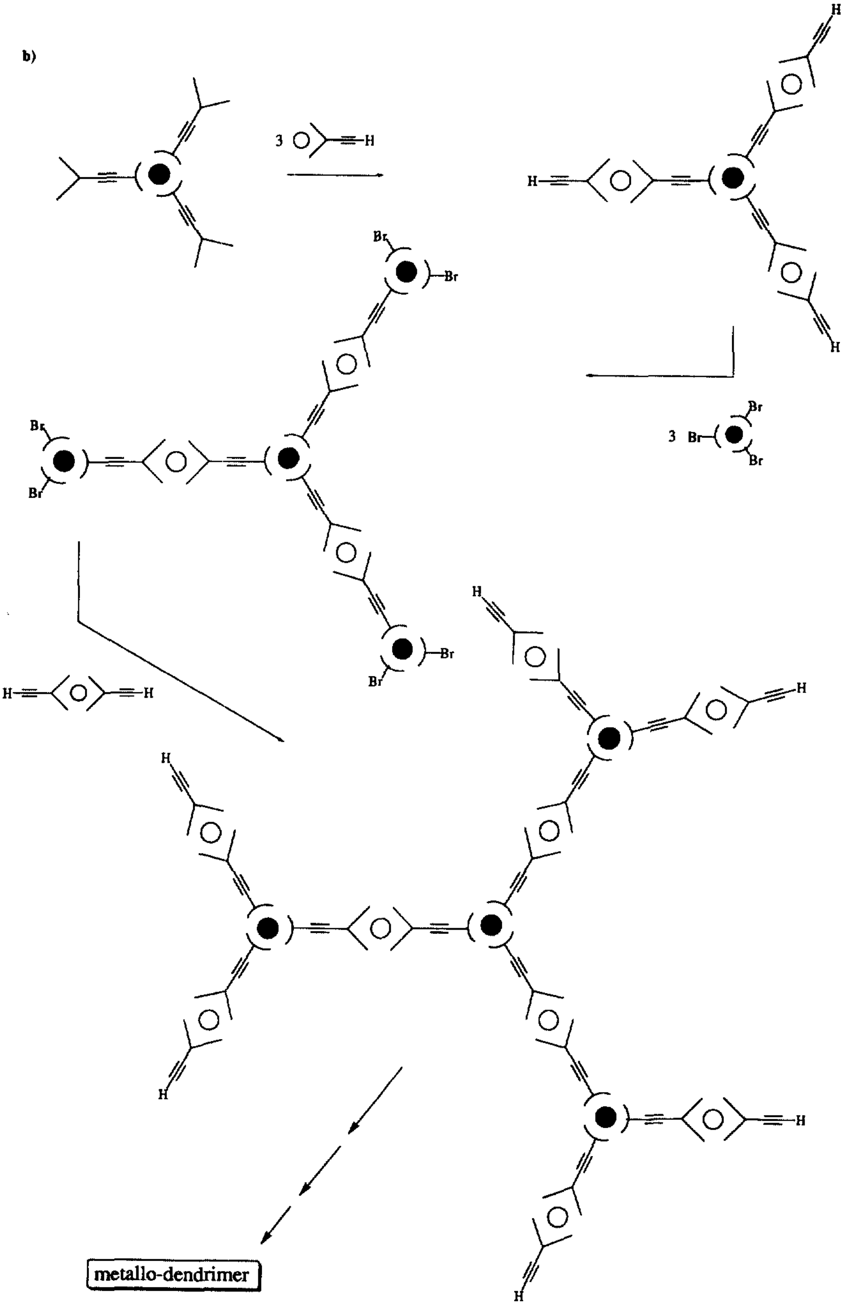

Fig. 38. (*continued*)

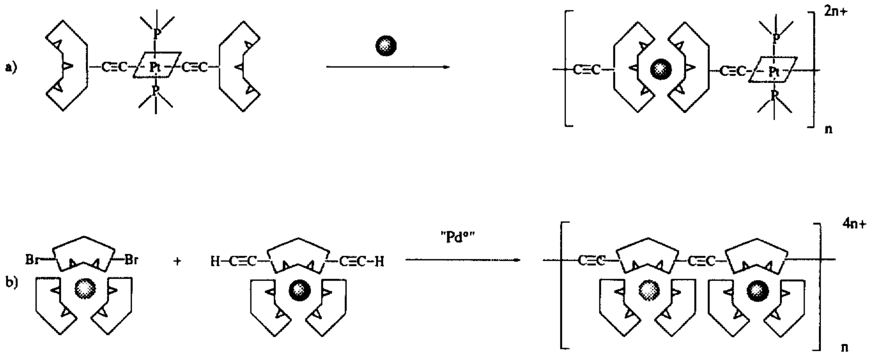

Fig. 39. Examples of the use of metallo-synthon building blocks for the preparation of linear metallo-polymers: (a) polymer built around a metal cation and (b) polymer obtained by a cross-coupling reaction between metallo-fragments bearing disparate functions.

phoric units either by selective metallo-polymerization [Fig. 39(a)] or by selective cross-coupling between metallo-synthon building-blocks [Fig. 39(b)]. These polymers are especially attractive candidates for non-linear optical materials and for liquid crystal display units.

13. Perspectives

Our laboratory is engaged in the design and synthesis of novel materials for use in future molecular-scale electronic devices. In this article we have outlined a strategy that permits the rational evocation of systems for which the extent of electron propagation along the molecular axis can be controlled to a rather fine tolerance. This is a major advance since, for the first time, it becomes possible to attenuate the rate of information transfer across an extended molecule to a predetermined extent. The power and simplicity of our approach is demonstrated by the realization that we can alter the rate of intramolecular triplet energy transfer between a given pair of reactants held at fixed separation distance by almost five orders of magnitude. Such variations are achieved not by changing the temperature or the thermodynamic parameters, but merely by introducing a particular relay into the molecular circuit. Furthermore, we have engineered molecular systems that can be fine-tuned to display selectivity and specificity for information transfer under external stimulation.

We are well aware, of course, that these molecular systems fall well short of functioning as a photoelectronic device. At present, there is no large-scale order in the system such that individual molecules act independently and without cooperation. While progress at the molecular level has been rapid, we have been less successful at the supramolecular level. This is where our future endeavors must concentrate. Already, we have learned how to form conductive films by electropolymerization of the alkyne function [91]. Related work has established ways to incorporate functionalized metal oligopyridine complexes into liquid crystalline materials [92,93] and into ferromagnetic order [94,95].

For the practitioner of molecular chemistry there is security in working with small molecules in fluid solution [96]. New materials are readily characterized and their properties are easily investigated. Theoretical principles abound by which to express structure reactivity criteria. There is the added glamor of being concerned with the fundamentals of the subject rather than being preoccupied with the tedium of making a practical device operate reliably. Even at the supramolecular level it is still possible to apply rigorous chemical principles to the characterization and study of new materials, provided the molecular weight of the emerging supermolecule remains manageable. Our goal for the immediate future is to extend our ideas to the formation of networks in which individual molecules act cooperatively to provide some degree of two-dimensional order. It should be possible, given our present state of knowledge, to design a molecular system that will self-organize into a cyclic cluster, somewhat reminiscent of the pigment arrays found in certain bacterial light-harvesting complexes [97]. We are looking, therefore, for ways to generate cyclic clusters containing seven or nine photoactive units interconnected by a conductive acetylenic bridge in order to develop a system capable of large-scale photon delocalization.

New molecules for new applications require new synthetic procedures. We have shown here that the use of metallo-synthons in stepwise Pd^0-catalyzed cross-coupling reactions allows the preparation of symmetrical or asymmetrical compounds that cannot be prepared by classical methods. Improved synthetic methods will be needed for the successful development of photoelectronic systems that operate at the supramolecular level. Consequently, we are working actively on the development of appropriate synthetic modalities, especially the identification of new metallo-synthons that display better selectivity for coordination to preferred ligands under mild conditions. Likewise, the biggest obstacle for our future development relates to the proper characterization of large arrays of identical chromophores held in place by functionalized acetylenic wires. X-ray crystallography remains the best analytical tool for such elaborate systems, but we are currently engaged in the development of alternative experimental tools that will provide crucial information about the structural integrity of our new supramolecular arrays.

Acknowledgements

We thank Dr. Andrew C. Benniston, Hélène Fleck, Dr. Vincent Grosshenny, Dr. Francisco M. Romero, and Olivier Trompette for their expert assistance during this research program. Financial support from the United States National Science Foundation, The Royal Society of London, Johnson Matthey plc, the Centre National de Recherche Scientifique, Université Louis Pasteur de Strasbourg, and the ECMP is gratefully acknowledged. We also thank Professor Hans Lami for providing access to cryogenic equipment and for his interest in this work. We are likewise indebted to the various analytical service laboratories at the Université Louis Pasteur and especially to Drs. André De Cian, Alain van Dorsselaer, and

Jean Fischer for providing specialist information. The Bruker Company kindly provided Pt NMR facilities. Some of the spectroscopic studies were made at the Center for Fast Kinetics Research (Austin, TX).

References

[1] A. Harriman, R. Ziessel, J. Chem. Soc., Chem. Commun. (1996) 1707.
[2] V. Grosshenny, A. Harriman, M. Hissler, R. Ziessel, Platinum Met. Rev. 40 (1996) 26.
[3] V. Grosshenny, A. Harriman, M. Hissler, R. Ziessel, Platinum Met. Rev. 40 (1996) 72.
[4] R. Ziessel, A. Harriman, Lettres de Départements Scientifiques du CNRS, Sciences Chimiques 55 (1996) 11.
[5] A.C. Benniston, A. Harriman, V. Grosshenny, R. Ziessel, New J. Chem. 21 (1997) 405.
[6] V. Grosshenny, A. Harriman, R. Ziessel, Angew. Chem., Int. Ed. Engl. 34 (1995) 1100.
[7] A. Helms, D. Heiler, G. McLendon, J. Am. Chem. Soc. 113 (1991) 4325.
[8] A. Helms, D. Heiler, G. McLendon, J. Am. Chem. Soc. 114 (1992) 6227.
[9] J. Onuchic, D.N. Beratan, J. Am. Chem. Soc. 109 (1987) 6771.
[10] P. Siders, R.J. Cave, R.A. Marcus, J. Chem. Phys. 81 (1984) 5613.
[11] A. Osuka, K. Marayama, N. Mataga, T. Asahi, I. Yamazaki, N. Tamai, J. Am. Chem. Soc. 112 (1990) 4958.
[12] L.R. Khundkar, A.E. Stiegman, J.W. Perry, J. Phys. Chem. 94 (1990) 1224.
[13] S. Woitellier, J.P. Launay, C.W. Spangler, Inorg. Chem. 28 (1989) 758.
[14] J.E. Sutton, H. Taube, Inorg. Chem. 20 (1981) 3125.
[15] A.E. Stigman, E. Graham, K.J. Perry, L.R. Khundkar, L.-T. Cheng, J.W. Perry, J. Am. Chem. Soc. 113 (1991) 7658.
[16] C. Dehu, F. Meyers, J.L. Brédas, J. Am. Chem. Soc. 115 (1993) 6198.
[17] J.O. Morley, J. Phys. Chem. 99 (1995) 10166.
[18] S. Priyadarshy, M.J. Therien, D.N. Beratan, J. Am. Chem. Soc. 118 (1996) 1504.
[19] J.L. Brédas, R. Silbey, D.S. Boudreaux, R.R. Chance, J. Am. Chem. Soc. 105 (1983) 6555.
[20] M.P. Samanta, W. Tian, S. Dutta, J.I. Henderson, C.P. Kubiak, Phys. Rev. B 53 (1996) 7626.
[21] A. Harriman, M. Hissler, R. Ziessel, A. De Cian, J. Fischer, J. Chem. Soc., Dalton Trans. (1995) 4067.
[22] V. Grosshenny, A. Harriman, M. Hissler, R. Ziessel, J. Chem. Soc., Faraday Trans. 92 (1996) 2223.
[23] H. Masai, K. Sonogashira, N. Hagihara, Bull. Chem. Soc. Jpn. 44 (1977) 2226.
[24] A. Harriman, R. Ziessel, Coord. Chem. Rev., in press.
[25] M. Hissler, R. Ziessel, J. Chem. Soc., Dalton Trans. (1995) 893.
[26] W. Beck, B. Niemer, M. Wieser, Angew. Chem., Int. Ed. Engl. 32 (1993) 923.
[27] H. Lang, Angew. Chem., Int. Ed. Engl. 33 (1994) 547.
[28] U.H.F. Bunz, Angew. Chem., Int. Ed. Engl. 35 (1996) 969.
[29] V. Grosshenny, R. Ziessel, J. Organomet. Chem. C19 (1993) 453.
[30] V. Grosshenny, R. Ziessel, J. Chem. Soc., Dalton Trans. (1993) 817.
[31] P.J. Kim, H. Masai, K. Sonogashira, H. Hagihara, Inorg. Nucl. Chem. Lett. 6 (1970) 181.
[32] H.B. Fyfe, M. Mlekuz, D. Zargarian, R. Taylor, T.B. Marder, J. Chem. Soc., Chem. Commun. (1991) 191.
[33] D. Péron, A. Romero, P.H. Dixneuf, Organometallics 14 (1995) 3319 and references cited therein
[34] W. Weng, T. Bartik, M. Brady, B. Bartik, J.A. Ramsden, A.M. Arif, J.A. Gladysz, J. Am. Chem. Soc. 117 (1995) 11922.
[35] R.W. Lass, P. Steinert, J. Wolf, H. Werner, Chem. Eur. J. 2 (1996) 19.
[36] G. Roth, H. Fischer, Organometallics 15 (1996) 1139.
[37] F. Coat, C. Lapinte, Organometallics 15 (1996) 477.
[38] T. Bartik, B. Bartik, M. Brady, R. Dembinski, J.A. Gladysz, Angew. Chem., Int. Ed. Engl. 35 (1996) 414.
[39] O. Lavastre, M. Even, P.H. Dixneuf, A. Pacreau, J.P. Vairon, Organometallics 15 (1996) 1530.

[40] V. Wing-Wah Yam, V. Chor-Yue Lau, K.-K. Cheung, Organometallics 15 (1996) 1740.
[41] V. Grosshenny, A. Harriman, R. Ziessel, Angew. Chem., Int. Ed. Engl. 34 (1995) 2705.
[42] V. Grosshenny, A. Harriman, R. Ziessel, Angew. Chem., Int. Ed. Engl. 33 (1994) 1884.
[43] S. Boyde, G.F. Strouse, W.E. Jones Jr., T.J. Meyer, J. Am. Chem. Soc. 112 (1990) 7395.
[44] G.F. Strouse, J.R. Schoonover, R. Duesing, S. Boyde, W.E. Jones Jr., T.J. Meyer, Inorg. Chem. 34 (1995) 473.
[45] A.J. Downard, G.E. Honey, L.F. Phillips, P.J. Steel, Inorg. Chem. 30 (1991) 2260.
[46] V. Grosshenny, A. Harriman, F.M. Romero, R. Ziessel, J. Phys. Chem. 100 (1996) 17472.
[47] M. Hissler, R. Ziessel, New J. Chem. 19 (1995) 751.
[48] V. Grosshenny, F.M. Romero, R. Ziessel, J. Org. Chem. 62 (1997) 1491.
[49] FörsterT., Discuss. Faraday Soc. 27 (1959) 7.
[50] D.L. Dexter, J. Chem. Phys. 21 (1953) 836.
[51] G.L. Closs, J.R. Miller, in: J.R. Norris, D. Meisel (Eds.), Photochemical Energy Conversion, Elsevier, New York, 1989, p. 23.
[52] R.A. Marcus, Discuss. Faraday Soc. 29 (1960) 21.
[53] V. Balzani, F. Bolletta, F. Scandola, J. Am. Chem. Soc. 102 (1980) 2152.
[54] L.G. Mackay, H.L. Anderson, J.K.M. Sanders, J. Chem. Soc., Chem. Commun. (1992) 43.
[55] K. Sonogashira, T. Yatake, Y. Tohda, S. Takahashi, N. Hagihara, J. Chem. Soc., Chem. Commun. (1977) 291.
[56] S. Takahashi, M. Kiraya, T. Yatake, K. Sonogashira, N. Hagihara, Macromolecules 11 (1978) 1063.
[57] B.F.G. Johnson, A.K. Kakkar, M.S. Khan, J. Lewis, A.E. Dray, R.H. Friend, F. Wittman, J. Mater. Chem. 1 (1991) 485.
[58] M. Hissler, R. Ziessel, New J. Chem. 21 (1997) 843.
[59] A.D. Hamilton, H.-D. Rubin, A.B. Bocarsley, J. Am. Chem. Soc. 106 (1984) 7255.
[60] J.L. Sessler, V.L. Capuano, A.K. Burrell, Inorg. Chim. Acta 204 (1993) 93.
[61] J.-P. Collin, A. Harriman, V. Heitz, F. Odobel, J.-P. Sauvage, J. Am. Chem. Soc. 116 (1994) 5679.
[62] A. Harriman, F. Odobel, J.-P. Sauvage, J. Am. Chem. Soc. 116 (1994) 5481.
[63] A. Harriman, F. Odobel, J.-P. Sauvage, J. Am. Chem. Soc. 117 (1995) 9461.
[64] A. El-ghayoury, R. Ziessel, Tetrahedron Lett. 38 (1997) 2471.
[65] D.N. Beratan, J.J. Hopfield, J. Am. Chem. Soc. 106 (1984) 1584.
[66] A. Harriman, J.-P. Sauvage, Chem. Soc. Rev. (1996) 41.
[67] S.M. Risser, D.N. Beratan, T.J. Meade, J. Am. Chem. Soc. 115 (1993) 2508.
[68] M. Hissler, O. Trompette, A. Harriman, R. Ziessel, submitted for publication.
[69] K. Mandal, T.D.L. Pearson, W.P. Krug, J.N. Demas, J. Am. Chem. Soc. 105 (1983) 701.
[70] M.R. Wasielewski, M.G. Johnson, W.A. Svec, K.M. Kersey, D.W. Minsek, J. Am. Chem. Soc. 110 (1988) 7219.
[71] H. Heitele, P. Finckh, S. Weeren, F. Pöllinger, M.E. Michel-Beyerle, J. Phys. Chem. 93 (1989) 5173.
[72] A. Harriman, V. Heitz, M. Ebersole, H. Van Willigen, J. Phys. Chem. 98 (1994) 4982.
[73] H.H. McConnell, J. Chem. Phys. 35 (1961) 508.
[74] R. Engelman, J. Jortner, Mol. Phys. 18 (1970) 145.
[75] A.M. Brun, A. Harriman, Y. Tsuboi, T. Okada, N. Mataga, J. Chem. Soc., Faraday Trans. 91 (1995) 4047.
[76] A. El-ghayoury, A. Harriman, R. Ziessel, in preparation.
[77] H. Heitele, M.E. Michel-Beyerle, P. Finckh, Chem. Phys. Lett. 134 (1987) 273.
[78] G.J. Wilson, W.H.F. Sasse, A.W.-H. Mau, Chem. Phys. Lett. 250 (1996) 583.
[79] P. Belser, R. Dux, M. Baak, L. De Cola, V. Balzani, Angew. Chem., Int. Ed. Engl. 34 (1995) 595.
[80] C. Weinheimer, Y. Choi, T. Caldwell, P. Gresham, OlmstedJ., III, J. Photochem. Photobiol. A 78 (1994) 119.
[81] G. Steinberg-Yfrach, P.A. Liddell, C.-C. Hung, A.L. Moore, D. Gust, T.A. Moore, Nature 385 (1997) 239.
[82] A. Otsuka, S. Nakajima, T. Okada, S. Taniguchi, K. Nozaki, T. Ohno, I. Yamazaki, Y. Nishimura, N. Mataga, Angew. Chem., Int. Ed. Engl. 35 (1996) 92.
[83] J.-C. Chambron, A. Harriman, V. Heitz, J.-P. Sauvage, J. Am. Chem. Soc. 115 (1993) 7419.
[84] V. Grosshenny, R. Ziessel, Tetrahedron Lett. 33 (1992) 8075.

[85] M. Hissler, A. Harriman, R. Ziessel, in preparation.
[86] M. Hissler, A. El-ghayoury, A. Harriman, R. Ziessel, Angew. Chem., Int. Ed. Engl. 38 (1998) in press.
[87] F. Barigelletti, L. Flamigni, M. Guardigli, J.-P. Sauvage, J.-P. Collin, A. Sour, Chem. Commun. (1996) 1329.
[88] F.R.M. Romero, A. Harriman, R. Ziessel, in preparation.
[89] D. Tzalis, Y. Tor, J. Chem. Soc., Chem. Commun. (1996) 1043.
[90] D. Tzalis, Y. Tor, J. Am. Chem. Soc. 119 (1997) 852.
[91] V. Grosshenny, A. Harriman, J.-P. Gisselbrecht, R. Ziessel, J. Am. Chem. Soc. 119 (1996) 10315.
[92] L. Douce, R. Ziessel, R. Seghrouchni, A. Skoulios, E. Campillos, R. Deschenaux, Liquid Cryst. 20 (1996) 235.
[93] A. El-ghayoury, L. Douce, R. Ziessel, R. Seghrouchni, A. Skoulios, Liquid Cryst. 21 (1996) 143.
[94] R. Ziessel, Mol. Cryst. Liq. Cryst. 273 (1995) 101.
[95] F.M. Romero, R. Ziessel, M. Drillon, J.-L. Tholence, C. Paulsen, N. Kyritsakas, J. Fischer, Adv. Mater. 8 (1996) 826.
[96] J.-L. Lehn, in: Supramolecular Chemistry, VCH, Weinheim, 1995.
[97] G. McDermott, S.M. Prince, A.A. Freer, A.M. Hawthornthwaite-Lawless, M.Z. Papiz, R.J. Cogdel, N.W. Isaacs, Nature 374 (1995) 517.